Root and canopy traits and adaptability genes explain drought tolerance mechanism in winter wheat.

Nehe, A.S.[1*], Foulkes M. J.[2], Ozturk, I.[1], Rasheed A.[3], York L.[4], Kefauver S.C.[5], Ozdemir F.[6]. Morgounov A.[7].

[1]International Maize and Wheat Improvement Center (CIMMYT), Ankara, Turkey.

[2]Division of Plant and Crop Science, School of Biosciences, University of Nottingham, UK.

[3]International Maize and Wheat Improvement Center (CIMMYT) China Office, Beijing, China.

[4]Noble research Institute 2510 Sam Noble Parkway Ardmore, OK 73401, US.

[5]Integrative Crop Ecophysiology Group, University of Barcelona, Spain.

[6]Bahri dagdas international agricultural research institute, Konya, Turkey.

[7]Omsk State Agrarian University, Institute Sq. 1, Omsk 644008 Russia

Abstract

Bread wheat (*Triticum aestivum* L) is one of main staple food crops worldwide contributing 20% calories in human diet. Drought stress is the main factor limiting yields and threatening to food security, with climate change resulting in more frequent and intense drought. Developing drought-tolerant wheat cultivars is a promising way forward. The use of a holistic approaches that include high-throughput phenotyping and genetic makers in selection could help in accelerating genetic gains. Fifty advanced breeding lines were selected from the CIMMYT Turkey winter wheat breeding program and studied under irrigated and semiarid conditions for two years. High-throughput phenotyping were done for wheat crown root traits using shovelomics techniques and canopy green area and senescence dynamics using vegetation indices (green area using RGB images and Normalized Difference Vegetation Index using spectral reflectance). In addition,

genotyping by KASP markers for adaptability genes was done. Overall, under semiarid conditions compared to irrigated conditions yield reduced by 3.09 t ha^{-1} (-46.8%). Significant difference between the treatment and genotype was observed for grain yield and senescence traits. Genotypes responded differently under drought stress. Root traits including shallower nodal root angle under irrigated conditions and root number per shoot under semiarid conditions were associated with increased grain yield. RGB based vegetation index measuring canopy green area at anthesis was more strongly associated with GY than NDVI under drought. Five established functional genes (*PRR73.A1* – flowering time, *TEF-7A* – grain size and weight, *TaCwi.4A* - yield under drought, *Dreb1*- drought tolerance, and *ISBW11.GY.QTL.CANDIDATE*- grain yield) were associated with different drought-tolerance traits in this experiment. We conclude that a combination of high-throughput phenotyping and selection for genetic markers can help to develop drought-tolerant wheat cultivars.

*Corresponding auther:ajit.nehe@gmail.com (NA)

Keywords: drought tolerance, root system architectural traits, vegetation index, canopy senescence, wheat.

1. Introduction

Wheat (*Triticum aestivum* L.) is one of the most important food crops contributing around 20% of calories in the human diet worldwide. However, climate change has resulted in more frequent and intense episodes of drought which affect wheat production (1). Worldwide drought

is the single most important factor affecting wheat yields (2) and model-based predictions indicate that there will be 9–12% wheat yield reduction in 21st century without considering the benefits of CO_2 fertilization and adaptations (3). Developing new drought-tolerant varieties is therefore important to achieve food security in the face of climate change. Identifying drought-tolerance traits for deployment in breeding is therefore crucial. Deeper root systems and cooler canopy temperature are two important traits reported to be responsible for drought tolerance in wheat (4,5). As roots are difficult to study under field conditions, canopy temperature has been applied as an indirect way of assessing the role of the root system as higher water transpiration and uptake is related to a cooler canopy. Canopy stay-green characters have also shown promise to help select drought-tolerance genotypes (6,7).

Wheat root systems consist of seminal roots (up to 6) and crown roots (around 10-15) per plant emerging from basal node of main shoots and tillers (8). These two root systems function together to acquire water and nutrients from the soil (9–11). Distribution of root length density (root length per unit soil volume; RLD) with depth is one of the important traits responsible for water capture in wheat crops (6,9,12). In synthetic wheat-derived lines, yield increase under water stress conditions was associated with increase in root dry weight at depth in NW Mexico (13). Higher allocation of plant assimilates to deeper roots was responsible for a cooler canopy and increase in overall grain yield under drought conditions in synthetic derived material (5). Narrower root angle in the top soil (steeper roots) was associated with higher root density in deeper soil in Australia (13–15).

The high-throughput phenotyping of root system architecture under the field conditions presents a bottleneck in breeding for drought tolerance in wheat (16). Previously, the soil-core break method (17) and ‘shovelomics’ (18) have been used for high-throughput field phenotyping

in cereals. Shovelomics, which mainly focuses on crown root phenotyping, involves the excavation of roots in the topsoil and measuring root traits manually or through image analysis. Using this method results of direct measurements and visual scoring in maize showed correlations with root depth for crown root number and angle (18). Shovelomics methods have quantified genetic variation in crown root angle and root length in maize (18–20), barley (21) and durum wheat (22). We used a high-throughput shovelomics technique for phenotyping root crown architecture of the whole root crown in wheat, as developed by (23).

The use of Normalized Difference Vegetation Index (NDVI) spectral reflectance index to study canopy growth and senescence dynamics has been common for decades, but it does have its limitations (24,25). Especially at high values of leaf area index (LAI), NDVI tends to saturate and does not show as strong of a linear association with yield components (26,27). Also, in order to obtain accurate results with NDVI, bright conditions with direct sunlight are required while taking the measurements (in the case of passive sensors). Senescence is a genetically programmed and environmentally influenced process (Thomas and Howarth, 2000) and the stay-green phenotype has shown proven utility to improve yields under drought (Borrell et al., 2000; Verma et al., 2004). NDVI has been used to measure stay green in wheat under drought (7). RGB image-based vegetation indexes have proved to be better associated with grain yield than NDVI under similar circumstances and also are time-saving (27).

Marker-assisted selection is very important component of molecular breeding to develop resilient cultivars by selecting and accumulating favorable alleles. In bread wheat several genes underpinning drought adaptability have been identified and molecular markers have been developed to select favorable alleles. However, the distribution and association of such functional genes like *Derb1*, *PRR-73*, *TaCwi-A1* and *TEF-7* is largely unknown in wheat cultivars from the

most parts of the world. Transcription factors like *DREB* known to control the expression of several functional genes responsible for plant tolerance to drought, high-salt and cold stress and have been propose to use in plant improvement for stress tolerance (28). Similarly, *TaTEF-7A* is transcript elongation factor gene responsible for number per spike (29) and thousand grain weight under (30). The gene *TaPRR73* was found to be regulation of flowering date and can be used in breeding to develop cultivars adaptable for different geographical areas (31). *TaCwi-A1* gene produce cell wall invertase enzyme manly responsible for sink tissue development and carbon allocation and showed affecting grain weight in wheat (32).

The present study reports associations between nodal root traits measured using the wheat shovelomics techniques along with vegetation indexes in a set of 50 CIMMYT Turkey winter wheat cultivars and advanced lines. The experiment was conducted under irrigated (IR) and semiarid (SA) field conditions in Turkey in two years. The germplasm was also screened for allelic variation of genes previously related to drought adaptability genes using breeder friendly KASP markers. Our aim was to identify genes and traits to use in winter wheat breeding for drought tolerance in Mediterranean region.

2. Materials and methods

2.1 Experimental design and plot management

Two field experiments were conducted at Bahri Dagdas International Agricultural Research Institute, Konya in 2017–18 and 2018–19. Before sowing the experimental field was fallow. The soil type was a sandy clay. Experiments were conducted in a randomized block, split–

plot design, in which two irrigation treatments (IR: drip-irrigated and SA: semiarid/rain-fed) were randomized on main-plots, and 50 CIMMYT winter wheat cultivars and advanced lines including 4 check cultivars were randomized on sub-plots in two replicates. The 50 winter wheat genotypes represent modern germplasm developed by International Winter Wheat Improvement Program and obtained from cooperators in Eastern Europe. They were selected on the basis of their performance under both irrigated and semiarid conditions in advanced cultivar trials. The check cultivars used were Gerek, Katea, Konya and Nacibey (S Table 1). Plots were 7.0 m × 1.2 m with 6 rows 20 cm apart and 450 seeds were sown per square meter. Fertilizers applied were 100 kg ha^{-1} of phosphorus (P) and 39 kg ha^{-1} of nitrogen (as ammonium nitrate) per hectare at the time of planting, and an additional 50 kg ha^{-1} of N at tillering (GS35). Under the irrigated treatment drip-irrigation was given as 50 mm application each time. Irrigation was given twice during the crop growth season at tillering and flowering stage.

2.2 Crop measurements: Grain yield and yield components

In 2018, a 1.5 m row bulk sample was hand-harvested by cutting at ground level at physiological maturity (GS89). The fertile shoots (those with an ear) were counted and 5 primary (large ear and stem) fertile shoots were selected for dry matter partitioning analysis. In 2019, around 10-20 shoots were selected for dry matter partitioning analysis from the sample for root measurements (next section). All selected shoots were separated into ears and straw. Dry weight of the ears and the straw was recorded after drying at 80^{o}C for 48 h. The ears of the bulk sample were then hand threshed and grain weighed. All grains were counted by a Contador seed counter (Pfeuffer, Germany) and 1,000 grain weight (TGW) was calculated. From these data the grain DM

per fertile shoot, harvest index (HI; grain DM / above-ground DM), fruiting efficiency (grain weight per ear dry weight) and above ground dry matter (AGDM; GY/HI) were calculated. The grain yield was calculated by weighing grain from rest of the plot which was machine-harvested (adjusted to 85% dry weight).

2.3 Shovelomics root crown trait measurements

The methodology for assessing root crown traits in both years was similar with some modification. Root crowns were excavated from all sub-plots during late-grain filling. A spade of 25 cm width and 30 cm depth was inserted to 20 cm depth on either side of plants keeping blade parallel to the row. Single sample were taken per plot. The soil was placed into a 10 L bucket filled with water for overnight. Next day root crowns sprayed with low pressure water from a hose to remove remaining soil. Three plant per sample where selected for scanning or image analysis. The number of fertile shoots for each of the three plants was counted. In 2018, root images were acquired and analyzed using WinRHIZO Regular V. 2009c scanner and software (Regent Instruments Inc., Canada). The traits measured were root surface area (cm^2), root diameter (mm), and root volume (cm^3). In 2019, images of the roots were taken with a RGB camera (Sony a 6000). A single image per sample was taken with auto setting. Roots were placed over black background to maximum contrast and sample ID and reference scale (white square of 2 cm x 1 cm) was placed on side of the roots as shown in S Fig. 1. Images were analyzed using a modified method from York and Lynch (33). A project for the ObjectJ plugin (https://sils.fnwi.uva.nl/bcb/objectj) for ImageJ (34) was created to allow the angles, numbers, stem diameter and roots diameter to be measured from the plant-root samples (S Fig. 1). The pixel dimensions were converted to physical

155 units using measurements of the known-sized scale in every image. The traits measured were root
156 number per shoot, root diameter (mm), and root angle (°). A polyline was used to measure the
157 crown lengths of the outermost roots and the seminal root length, and the angle was measured for
158 the outermost crown roots at approximately 5 cm depth by measuring the width then later
159 calculating angle using trigonometry and the actual depth measurement to where width was
160 measured. For nodal root number, each nodal root axis was manually annotated, and the count
161 recorded in an output file. The image analysis gave values for the number of pixels corresponding
162 to root diameter and numbers. Using the 2 cm x 1 cm reference square, these pixel values were
163 then converted to the relevant units for each root measurement in excel that also calculated angles
164 as detailed in (33).

165

166 2.4 NDVI and RGB based vegetation indexes and canopy temperature

167 In 2018, Normalized Difference Vegetation Index (NDVI) was measured using the
168 handheld active sensor Trimble GreenSeeker spectroradiometer (Trimble Navigation Ltd, USA)
169 to assess the canopy green area starting from booting (GS41). Modified Gompertz curves (Eq. 1)
170 were fitted to the NDVI values against thermal time (base temp. 0^{o}C after anthesis, GS61, Zadoks
171 et al., 1974). The Gompertz (T) parameter was fitted as the thermal time for the NDVI to decrease
172 to 37% NDVI value at GS61. The thermal time (t, measured in °CD) when NDVI values were
173 90% and 10% of the value at GS61 were taken as the onset of senescence (SenSt) and end of
174 senescence (SenEnd), respectively, whereas the duration from 90% NDVI to 10% NDVI
175 remaining was considered as the senescence duration (SenDu).

176 $$Y = K * \exp\{-\exp((t-T)*2/D)\}$$ Equation 1

where t is thermal time (base temp. 0°C), D is duration of senescence (SenDu), T is the timing of the inflection point at 37% NDVI value remaining from initial point at GS61, K value is the maximum NDVI at GS61. The senescence parameters were estimated for each sub-plot and then subjected to ANOVA.

In 2019, RGB images and NDVI (GreenSeeker Trimble Navigation Ltd, USA) were taken every two weeks from tillering (GS35) to crop maturity (GS89). RGB image-based vegetation index - green area per meter square (GA m^{-2}) was calculated using equation 2 to 6:

$$GSD = (SW \times H) / (FL \times IW) \quad \text{Equation 2}$$

$$DW = GSD \times IW \quad \text{Equation 3}$$

$$DH = GSD \times IH \quad \text{Equation 4}$$

$$A = DW \times DH \quad \text{Equation 5}$$

$$\text{Green area } m^{-2} = GA \times A \quad \text{Equation 6}$$

whereas GSD is ground sampling distance (centimeters/pixel), SW is camera sensor width (mm), H is camera height from top of the canopy (m), FL is focal length of camera (mm), DW is width of single image footprint on the ground (m), DH is height of single image footprint on the ground (m), IW is image width (pixels), IH is image height (pixels), A is ground area in image (m^2) and GA is index value output after image analysis using BreedPix. BreedPix is open source software (35), implemented as part of the open-source CerealScanner plugin (Fernandez-Gallego et al., 2019, https://gitlab.com/sckefauver/cerealscanner) developed for ImageJ software (34). Green Area per meter square at anthesis (GA An) and 2 weeks after anthesis (GA 2W) values are

198 used in this paper. Canopy temperature was measured at anthesis using handheld infrared
199 temperature meter (SBRMART GM320).

200

201 ## 2.5 Genotyping

202 DNA was extracted from all genotypes using a modified CTAB method (36). Allele-
203 specific KASP markers for five different loci were used. The primer sequences and amplification
204 conditions of each gene are described in Khalid et al. (2019). The detailed genotyping procedures
205 have been described elsewhere (37,38). Briefly, two allele-specific primers carrying standard FAM
206 tail (5′-GAAGGTGACCAAGTTCATGCT-3′) and HEX tail (5′-
207 GAAGGTCGGAGTCAACGGATT-3′), with targeting SNP at the 3′end, and a common reverse
208 primer were synthesized. The primer mixture included 46 µl ddH_2O, 30 µl common primer (100
209 µM) and 12 µl of each tailed primer (100 µM). Assays were tested in 384-well format and set up
210 as 5 µl reaction [2.2 µl DNA (10–20 ng/µl), 2.5 µl of 2XKASP master mixture and 0.056 µl primer
211 mixture]. PCR cycling was performed using the following protocol: hot start at 95°C for 15 min,
212 followed by ten touchdown cycles (95°C for 20 s; touchdown 65°C–1°C per cycle 25 s) further
213 followed by 30 cycles of amplification (95°C for 10 s; 57°C for 60 s). The extension step is
214 unnecessary as amplicon is less than 120 bp. The plate was read in BioTek H1 system and data
215 analysis was performed manually using Klustercaller software (version 2.22.0.5; LGC Hoddesdon,
216 United Kingdom).

217

218 ## 2.6 Marker-traits association analysis

In this paper we presented results of five key KASP markers out of 150 for their association with phenotypes (Table 5). These markers are regularly used in marker-assisted selection in CIMMYT's wheat breeding program. As some of the traits that we measured differed between years, the marker-traits associations (MTAs) were identified separately for each year. KASP markers for which one of the alleles was represented at relatively higher frequency (>80%) than other alleles were not considered for MTA. MTA analysis was done in R using liner model (lm) function (Eq. 7) to see the significant effect of the marker on traits by comparing the mean. BLUEs (best linear unbiased estimator) were calculated using Meta-R for randomized block design for all the traits for individual years. BLUE values were used to see the significant effect of marker on traits using following liner model.

$$Y_{jk} = \mu + M_j + G_k\,(M_j) \qquad \text{Equation 7}$$

Y is phenotyping value, μ is mean of the population, M is mean effect of j^{th} marker, $G_k(M_j)$ genotype within marker variance (error variance).

2.7 Statistics

In both years, GenStat 19th edition (VSN International, Hemel Hempstead, UK) was used for carrying out analysis of variance (ANOVA) of traits applying a split-plot design with replications regarded as random effects and genotypes as a fixed effect, and the least significant difference (LSD) test was used to compare the means between specific treatments. A cross-year ANOVA was applied to analyze irrigation treatments and genotypes effects across years and the interaction with year, assuming irrigation treatments and genotypes were fixed effects and replicates and year were random effects. Pearson's correlation coefficient (r) and linear regressions

coefficient (R^2) were calculated to quantify associations between traits for individual year and cross year means using GenStat. Principal component analyses were done to produce biplots using R software package "factoextra."

Table 1. Environmental conditions during two field crop growing seasons (2018 and 2019) at experimental site Konya, Turkey. Monthly temperature means, (minimum, maximum) and monthly rainfall.

	2017-18		2018-19	
	Temperature (°C) Mean (Min, Max)	**Rainfall (mm)**	**Temperature (°C) Mean (Min, Max)**	**Rainfall (mm)**
Nov	12.2 (-0.36, 12.5)	70.0	6.52 (0.92, 12.1)	27.4
Dec	7.60 (-2.02, 9.6)	18.6	3.29 (-0.47, 7.05)	63.4
Jan	3.22 (-2.66, 5.88)	4.60	0.75 (-3.92, 5.44)	66.6
Feb	11.9 (-0.35, 12.2)	0.20	4.25 (-0.99, 9.49)	31.6
Mar	19.7 (1.86, 17.7)	36.0	6.24 (-0.78, 13.3)	20.8
Apr	26.8 (4.95, 21.8)	14.4	9.59 (2.63, 16.5)	32.0
May	35.0 (9.45, 25.5)	72.2	17.12 (7.98, 26.2)	10.2
Jun	41.7 (12.3, 29.3)	38.8	21.23 (13.4, 29.0)	45.6
Jul	48.8 (16.6, 32.2)	20.4	22.76 (15.3, 30.1)	7.60
Total		**275.2**		**305.2**

3. Results

3.1 Drought effects on plant growth

Averaging across the 50 genotypes, the drought/semiarid (SA) conditions reduced the grain yield (GY) compared to irrigated (IR) conditions by 2.67 t ha^{-1} (-50.1%) in 2018 and 3.51 t ha^{-1} (-44.6%) in 2019 ($P < 0.001$; Table 2) with an average reduction over two years of 3.09 t ha^{-1} (-46.8%, P=0.01, Fig. 1). The cross-year ANOVA showed a significant Year x Genotype (Y x G) interaction ($P<0.001$, Table 2). Relative loss in GY under SA conditions ranged from -36.1% (genotype code no. 32) compared to -58.5% (genotype 9). The three-way interaction of Y x T x G (Year x Treatment x Genotype) was not significant.

257 Regression analysis showed a positive association amongst the genotypes for GY between
258 IR and SA conditions (R^2=0.27, P<0.001, Fig. 1 a). Nevertheless, some genotypes changed
259 rankings markedly; for example: genotype 33 dropped from 2nd highest under IR to 13th highest
260 under SA conditions; 16 and 25 also changed rankings with relatively higher rankings under SA
261 conditions than IR conditions (Table S2). GY also showed positive association with AGDM (IR:
262 R^2=0.21, P<0.001 and SA: R^2=0.22., P<0.001) and NDVI at anthesis (IR: R^2=0.18, P=0.01 and
263 SA: R^2=0.23., P<0.001) under both IR and SA conditions (Fig. 2 a and c).

264 For harvest traits, averaging across years, overall the AGDM was the component affected
265 most by the semiarid conditions reducing from 19.7 to 12.1 t ha^{-1} (-38.6%, P=0.01, Table 2);
266 whereas thousand grain weight (TGW) reduced from 36.6 to 32.1 (-12.2%, P=0.03, Table 2). For
267 AGDM, T x G interaction was not significant whereas for TGW it was (P=0.03). Reduction in
268 grains per ear under SA conditions ranged from -0.5% (genotype 16) to -49.0% (genotype 9).
269 Variation in response to drought for TGW was from -0.9 to -25.7%. Heading date (HD) was
270 advanced by two days in SA conditions compared to IR (P=0.004). There was a negative
271 association between GY and HD amongst cultivars under SA conditions (R^2=0.18, P=0.002), but
272 no association under IR conditions (Fig. 2 c). Overall drought reduced plant height by 31.6% but
273 there was no association between GY and PH amongst cultivars under either SA or IR conditions.
274 Harvest index showed a positive association with GY under IR (R^2=0.39, P<0.001) and SA
275 (R^2=0.28, P<0.001) conditions (Fig. 2 b).

276

277 **Figure 1**: Linear regression among the 50 winter wheat genotypes for (a) grain yield in semiarid on GY in
278 irrigated conditions (mean across the years) and (b) GY in 2018 on GY in 2019 under Irrigated (IR) and
279 semiarid (SA) conditions.

Table 2. Yield components traits for 50 CIMMYT winter wheat genotypes for 2018, 2019 and cross-year means (CY). Grain yield (GY t ha^{-1}), above ground dry matter (AGDM t ha^{-1}), harvest index (HI), plant height (PH cm), days to heading (HD), thousand grain weight (TGW), and fruiting efficiency (FE grains g^{-1}).

	GY t ha^{-1}		BM t ha^{-1}		HI		PH cm		HD		TKW g		FE grains g^{-1}	
Genotype	**IR**	**SA**	**IR**	**SA**	**IR**	**SA**	**IR**	**SA**	**IR**	**SA**	**IR**	**SA**	**IR**	**SA**
Mean 2018	5.33	2.67	12.9	5.97	0.42	0.30	86.5	52.4	122	121	37.3	35.8	19.4	15.4
Min 2018	4.22	1.61	9.9	3.57	0.30	0.23	70.5	39.0	118	118	23.4	28.2	14.3	10.4
Max 2018	6.56	3.76	17.5	8.88	0.48	0.36	98.0	63.5	129	128	50.5	44.2	26.4	19.6
Mean 2019	7.94	4.37	26.6	18.0	0.43	0.25	84.9	63.4	194	191	33.5	30.7	21.9	15.3
Min 2019	6.16	2.55	21.5	13.0	0.27	0.17	73.0	50.0	186	186	25.1	24.2	17.1	11.1
Max 2019	9.62	5.77	35.0	24.0	0.52	0.31	96.0	74.0	201	196	39.6	38.5	26.8	18.6
CY Mean	**6.61**	**3.51**	**19.7**	**12.1**	**0.36**	**0.34**	**83.7**	**57.3**	**182**	**180**	**36.6**	**32.1**	**17.4**	**18.6**
CY Min	5.25	2.48	16.8	9.2	0.28	0.23	72.1	46.8	176	176	26.6	25.7	14.5	14.8
CY Max	7.81	4.37	23.8	15.9	0.41	0.40	94.6	68.2	188	186	45.7	37.7	21.4	22.2
	LSD		LSD		LSD		LSD		LSD		LSD		LSD	
G (Genotype)	0.70	***	2.95	**	0.04	***	4.20	***	1.40	***	2.81	***	1.86	***
T (Treatment)	1.47	**	2.9	**	0.01	*	7.60	**	0.50	***	3.84	*	1.80	
Y (Year)	0.60	***	2.24	***	0.05	**	5.50	*	1.50	***	1.27	*	1.25	***
T*G	1.27		4.35		0.06		7.10	*	1.90	**	4.38	*	2.74	**
Y*G	1.02	***	4.25		0.06	*	6.50		2.10	***	3.98	***	2.67	***

Significance levels displayed as ns > .05, * <.05 >.01, ** <.01, ***<0.001.

Figure 2: Linear regression amongst 50 wheat genotypes between GY and (a) above ground dry matter (AGDM) (b) harvest index and (c) Heading date (DAS) under irrigated (IR) and semiarid (SA) conditions (mean of 2018 and 2019).

3.2 Root system traits and correlations with yield and yield components

In 2018, root traits were not significantly affected by the irrigation treatment. However, differences between the genotypes were observed in all the root traits ($P<0.05$, Table 3). Overall root surface area ranged from 28.4 to 59.4 cm^2 per plant with mean of 44.3 cm^2 per plant and 22.9 to 60.1 cm^2 per plant with mean of 43.4 cm^2 per plant under IR and SA conditions respectively.

296 Interestingly under SA conditions, GY and AGDM showed negative association with root surface
297 area (r = -0.29 and r = -0.32), and root volume (r = -0.26 and r = -0.28). However, TGW showed
298 positive association with root surface area (r = 0.40), root diameter (r = 0.52), and root volume (r
299 = 0.49). Under IR conditions root diameter and TGW showed positive association with GY (r =
300 0.27, and r = 0.29 respectively). Also, under IR conditions onset of senescence showed a positive
301 association with root diameter (r = 0.29, Table 5).

302 In 2019, root diameter (RoDiM), root number per plant (RoNoPl) and root:shoot ratio
303 (Ro:Sh ratio) showed significant differences between genotypes and treatments (Table 4). Overall
304 phenotypic variation amongst genotypes for root angle was from 46.7° to 68.0° with mean of 56.6°
305 and 46.1° to 63.8° with mean of 56.3° under IR and SA conditions, respectively. Root number per
306 shoot (RoNoSh) showed a positive association with GY and HI (r = 0.32 and r = 0.35, respectively)
307 under SA conditions but there was no association under IR conditions (Table 5). AGDM showed
308 a negative association with root diameter (r = -0.29) and root dry weight per plant (r = -0.49) under
309 IR conditions. Wider root angle was also associated with higher GY and AGDM under IR
310 conditions (r = 0.29 and r = 0.33, respectively; Table 6). Narrower root angle was associated with
311 more roots per plant under SA conditions, whereas under IR conditions these associations were
312 not significant. Root dry weight per plant also showed a positive association with root diameter
313 under IR conditions. There was a strong positive association between root dry weight and root
314 number per plant under both SA and IR conditions.

Table 3. ANOVA showing significance for genotype (G), treatment (T), interaction (G x T) and genetic ranges for root and senescence traits: root surface area (RoSuAr), root diameter (RoDiM), root volume (RoVol), NDVI at anthesis (NDVI), senescence start (SenSt), senescence duration (SenDu) in 2018.

	RoSuAr (cm2)		RoDiM (mm)		RoVol (cm^{-3})		NDVI		SenSt (°CD)		SenDu (°CD)	
	IR	SA	IR	SA	IR	SA	IR	SA	IR	SA	IR	SA
Mean	44.3	43.4	0.52	0.51	0.57	0.56	0.63	0.52	648	250	1001	1501
Min	28.4	22.9	0.42	0.41	0.31	0.24	0.56	0.40	425	149	669	1131
Max	59.4	60.1	0.69	0.64	0.86	0.87	0.71	0.61	1033	461	1401	2221
%red		2.17		1.36		2.82		17.6		61.4		-49.9
LSD												
G	11.6***		0.08***		0.19***		0.56***		127***		243***	
T	32.6		0.25		0.13		1.45 T		114**		8.43***	
T x G	17.13		0.12		0.26		0.82*		179***		341***	

Significance levels displayed as ns>.10, T <.10 & > .05, * <.05 >.01, ** <.01, ***<0.001.

Table 4. ANOVA showing significance for genotype (G), treatment (T), interaction (G x T) and genetic ranges for root and senescence traits: root angle (RoAng), root diameter (RoDiM), root dry weight per plant (RoDrWtPl), root number per plants (RoNoPl), root:shoot ratio (Ro:Sh Ratio), canopy temperature (CT), canopy green area per meter square at anthesis (GA) and NDVI at anthesis (NDVI) studied in 2019.

	RoAng (°)		RoDiM (mm)		RoDrWtPl (g)		RoNoPl		Ro:Sh Ratio		CT (°C)		GA		NDVI	
	IR	SA	IR	SA	IR	SA	IR	SA	IR	SA	IR	SA	IR	SA	IR	SA
Mean	56.6	56.3	0.71	0.68	0.52	0.49	19.9	15.2	0.08	0.06	29.3	36.9	1.94	1.68	0.72	0.57
Min	46.7	46.1	0.46	0.50	0.15	0.20	13.8	10.8	0.03	0.02	26.0	31.5	1.82	1.43	0.64	0.46
Max	68.0	63.8	0.87	0.79	0.99	0.99	27.0	23.3	0.17	0.10	32.0	43.0	2.00	1.90	0.79	0.66
%red		0.51		4.54		6.62		23.9		27.6		-26.2		13.1		20.8
LSD																
G	9.09		0.13*		0.32		5.28*		0.04 T		4.19		0.13**		0.06***	
T	1.82		0.03**		0.06		1.06***		0.01***		0.84***		0.02***		0.01***	
T X G	12.9		0.18		0.45		7.47		0.05		5.93		0.19		0.08*	

Significance levels displayed as ns>.10, T <.10 & > .05, * <.05 >.01, ** <.01, ***<0.001.

Table 5. Correlation matrix showing correlation coefficient (r) values for grain yield (GY), above ground dry matter (AGDM), harvest index (HI), thousand grain weight (TGW), heading date (HD), root surface area (RoSuAr), root diameter (RoDiM), root volume (RoVol), NDVI at anthesis (NDVI), NDVI senescence start (SenSt), NDVI senescence duration (SenDu). Below diagonal IR and above diagonal SA for 2018.

	GY	AGDM	HI	TGW	HD	RoSuAr	RoDiM	RoVol	NDVI	SenSt	SenDu
GY	- -	0.87 ***	0.51 ***	0.04	-0.35**	-0.29*	-0.08	-0.26 T	0.34**	0.14	-0.10
AGDM	0.72 ***	- -	0.03	-0.02	-0.30*	-0.32*	-0.10	-0.28*	0.23	0.03	0.02
HI	0.21	-0.51 ***	- -	0.09	-0.25 T	-0.05	0.00	-0.05	0.27 T	0.26 T	-0.25 T
TGW	0.29*	-0.01	0.40**	- -	-0.18	0.40**	0.52 ***	0.49 ***	0.01	0.01	0.07
HD	-0.11	0.18	-0.38**	-0.28*	- -	0.20	-0.14	0.12	0.10	-0.14	-0.14
RoSuAr	0.02	0.03	0.02	0.23	0.31*	- -	0.37**	0.91 ***	-0.06	-0.07	0.11
RoDi	0.27*	0.11	0.16	0.43***	-0.23	0.16	- -	0.68 ***	-0.12	0.03	0.04
RoVo	0.16	0.09	0.10	0.43**	0.13	0.84 ***	0.65 ***	- -	-0.09	-0.03	0.09
NDVI	0.34**	0.36**	-0.07	-0.03	0.26 T	-0.03	-0.14	-0.08	- -	0.48 ***	-0.63 ***
SenSt	0.38**	0.30*	0.03	0.35**	-0.33*	0.08	0.29*	0.20	-0.16	- -	-0.76 ***
SenDu	-0.27*	-0.17	-0.05	-0.25T	0.11	-0.16	-0.26 T	-0.25T	0.13	-0.74 ***	- -

Significance levels displayed as ns>.10, <.10 T > .05, * <.05 >.01, ** <.01, ***<0.001.

Table 6. Correlation matrix showing correlation coefficient (r) values for grain yield (GY), above ground dry matter (AGDM), harvest index (HI), thousand grain weight (TGW), days to heading (DH), canopy green area per meter square at anthesis (GA An) and after 2 weeks of anthesis (GA 2W), NDVI at anthesis (NDVI), root angle (RoAng), root diameter (RoDiM), root dry weight per plant (RoDrWtPl), root number per shoot (RoNoSht), and canopy temperature at anthesis (CT). Below diagonal IR and above diagonal SA for 2019.

	GY	AGDM	HI	TGW	HD	GA An	GA 2W	NDVI	RoAng	RoDiM	RoDrWtPl	RoNoSht	CT
GY	- -	0.34*	0.62 ***	0.51 ***	-0.40**	0.56 ***	0.76***	0.55 ***	0.11	-0.06	-0.01	0.32*	-0.28*
AGDM	0.43**	- -	-0.51 ***	-0.08	-0.18	0.04	0.10	0.01	0.10	0.02	-0.07	-0.06	-0.15
HI	0.37**	-0.60 ***	- -	0.55 ***	-0.22	0.44**	0.59***	0.47***	0.00	-0.07	0.06	0.35**	-0.15
TGW	0.16	-0.20	0.22	- -	-0.31*	0.16	0.40**	0.25 T	0.06	0.05	0.02	0.27T	-0.15
HD	-0.33*	-0.34*	0.17	-0.12	- -	0.12	0.05	0.01	-0.04	-0.21	0.06	-0.06	-0.07
GA An	0.36**	-0.01	0.42**	-0.25 T	0.26 T	- -	0.74***	0.86 ***	-0.12	-0.12	0.02	0.10	-0.39**
GA 2W	0.25T	0.08	0.28*	-0.17	0.27*	0.89***	- -	071***	0.15	-0.04	0.02	0.35**	-0.42**
NDVIAn	0.26 T	0.02	0.36**	-0.18	0.39**	0.69 ***	0.74***	- -	-0.02	-0.08	-0.05	0.03	-0.31*
RoAng	0.29*	0.33*	-0.08	-0.15	-0.02	-0.01	-0.09	0.27 T	- -	-0.08	-0.41**	-0.01	-0.12
RoDiM	-0.11	-0.29*	0.11	0.20	0.18	-0.04	0.08	0.18	0.05	- -	0.04	0.16	0.00
RoDrWtPl	-0.19	-0.49 ***	0.35*	0.26 T	0.27T	0.08	0.20	0.13	-0.25 T	0.34*	- -	-0.06	-0.08
RoNoSht	-0.15	0.06	-0.15	-0.05	0.33*	-0.03	-0.13	-0.02	-0.04	0.10	-0.07	- -	-0.18
CT	0.07	0.00	-0.07	0.11	-0.17	-0.27 T	-0.21	-0.17	0.10	0.18	-0.18	0.00	- -

Significance levels displayed as ns>.10, <.10 T > .05, * <.05 >.01, ** <.01, ***<0.001.

335 ## 3.3 Canopy senescence and temperature traits

336 Overall, in 2018 NDVI at anthesis (NDVI, GS61) ranged from 0.56 to 0.71 and 0.40 to
337 0.61 under IR and SA conditions, respectively. ANOVA shows that there was a significant
338 difference between genotypes and irrigation treatments along with significant G x T interaction
339 for NDVI at anthesis, senescence start (SenSt) and senescence duration (SenDu) (Table 3). There
340 was a positive association between NDVI at anthesis and GY under both, IR (r = 0.34) and SA (r
341 = 0.34) conditions (Table 5). Under IR conditions, NDVI at anthesis and senescence start (SenSt)
342 showed positive associations with GY (r = 0.34 and r = 0.38, respectively) whereas senescence
343 duration (SenDu) showed negative association with GY (r = -0.27) (Table 5).

344 In 2019, NDVI at anthesis ranged from 0.64 to 0.79 with mean of 0.72 and 0.46 to 0.66
345 with mean of 0.57 under IR and SA conditions, respectively. There was significant difference
346 between genotypes and treatments for canopy green area per meter square at anthesis and NDVI
347 at anthesis. G x T interaction was significant only for NDVI at anthesis (Table 4). In terms of
348 association between GY and vegetation indexes, canopy green area per meter square at anthesis
349 showed better association with GY than NDVI at anthesis and these associations were stronger
350 under SA (r = 0.56 and r = 0.55, respectively) conditions than IR (r = 0.36 and r = 0.26,
351 respectively) conditions (Table 6, Fig. 3). Under SA conditions both canopy green area at anthesis
352 and NDVI at anthesis showed a negative correlation (r = -0.39 and r = -0.31, respectively) with
353 canopy temperature (Table 6; Fig. 3). Canopy green area and NDVI after two and three weeks of
354 anthesis was not associated with GY.

355

356 **Figure 3:** Linear regression amongst 50 wheat genotypes between GY and (a) NDVI at anthesis (b) Green
357 area per meter square (GA) at anthesis under irrigated (IR) and semiarid (SA) conditions (mean of 2018
358 and 2019) at anthesis in 2019.

359

360 3.4 Association between different yield components under IR and SA condition:

361 Under IR conditions, the first principal component (PC1) explained 25.3% variation and
362 the group of traits explaining this variation were fruiting efficiency, spikelet's per ear, days to
363 heading with positive effect whereas TGW showed negative effect. The second principal
364 component (PC2) explained 20.8% variation and the group of traits explaining this variation
365 included grains per ear, harvest index, grain yield, and root diameter with positive effects whereas
366 above ground dry matter showed negative effects.

367 Under SA conditions, PC1 explained 25.6% variation and trait associated with positive
368 effect - were grains per ear, harvest index, grain yield, and NDVI whereas days to heading had
369 negative effects. PC2 explained 21.0% of variation and traits showing association with positive
370 effects were - thousand grain weight, plant height, root diameter, whereas spikelet's per ear had
371 negative effect (Fig. 4).

372

373 **Figure. 4:** Bi-plot for grain yield (GY), above ground dry matter (AGDM), harvest index (HI), thousand
374 grain weight (TGW), days to heading (DH), grain numbers per ear (GrEr), spikelet number per ear (SpEr),
375 fruiting efficiency at harvest (FE), NDVI at anthesis (NDVI) and root diameter (RoDiM) under irrigated
376 and semiarid conditions for 50 cultivars (Mean of 2018 and 2019).(Contrib: contribution in total variation
377 in per cent – red to blue: stronger to low).

3.5 Marker-traits associations

Marker, allele/haplotype effect, mean of traits for each allele and probability of significant difference in the mean under IR and SA conditions are presented in Table 7 for 2018 and 2019. In 2018, marker-trait analysis showed that marker *TaCwi-4A* have significant influence on GY under SA. This marker was responsible for increase in GY by 17.1% under SA in presence of Hap-4A-C allele which is responsible for higher yield under drought conditions (32) and present in 59% of genotypes. Marker *Dreb1* was responsible for increase root surface area (RoSuAr) and root volume (RoVol) only under SA conditions. *Dreb1* allele *TaDreb-B1a* increased these traits by 9.4% and 13.3%, respectively, under SA conditions. *Dreb1* was also associated with extended SenEnd under SA conditions. The *PRR73-A1* gene had a significant influence on GY under SA but not under IR conditions. There was an increase of 14.1% under SA conditions in presence of Hap-II allele which was present in 29% of genotypes studied. This allele was also associated with extended senescence end (SenEnd) under SA and IR conditions.

The marker-trait associations in 2018 were not apparent for the same traits in 2019. However, Marker *PRR73-A1* with allele Hap-I (early flowering) was responsible for increase above ground biomass at anthesis (AGBMAn; data not shown) and root: shoot ratio (Ro:Sh Ratio).

Table 7. The key markers and haplotype mean for traits: grain yield (GY t ha^{-1}), harvest index (HI), plant height (PH cm), thousand grain weight (TGW g), heading date (HD DAS), root surface area (RoSuAr cm^2), root diameter (RoDiM mm), root volume (RoVol cm^3), NDVI senescence end (SenEnd °CD), NDVI Mid senescence (MidSen °CD), canopy green area per meter square at anthesis (GA m2), root angle (RoAng °), root dry weight per plant (RoDrWtPl g), root shoot ratio (Ro:Sh ratio), and canopy temperature (CT °C)

under SA and IR conditions along with significant difference between the two haplotype mean to show marker-trait association in 2018 and 2019 for 50 genotypes.

		PRR73.A1		**TEF.7A**		**TaCwi.4A**		**Dreb1**		**GY.QTL**	
	Hap-I	Early flowering		Low TGW		Drought tolerant		Drought tolerant		High yield	
	Hap-II	Late flowering		High TGW		Drought susceptible		Drought susceptible		Low yield	
		SA	**IR**	**SA**	**IR**	**SA**	**IR**	**SA**	**IR**	**SA**	**IR**
2018											
GY	Hap-I	2.44*	5.27 T	2.66**	5.33	2.75**	5.41	2.49	5.33	2.40 T	5.29
	Hap-II	2.84	5.56	2.14	5.35	2.28	5.22	2.61	5.36	2.72	5.39
TGW	Hap-I	33.3	36.8	33.6	37.4	34.3 T	38.3	33.6	37.9	32.6*	36.6
	Hap-II	34.3	38.7	33.2	36.7	32.6	36.2	33.3	36.9	34.5	38.0
HD	Hap-I	121 T	123**	121*	122	121 T	122	121	122	121	122
	Hap-II	120	121	122	123	122	123	121	122	121	122
HI	Hap-I	0.42	0.41	0.43	0.42	0.43	0.42	0.41	0.41	0.43	0.42
	Hap-II	0.44	0.42	0.42	0.42	0.42	0.42	0.44	0.42	0.42	0.41
PH	Hap-I	51.3*	85.3*	53.1 T	86.2	53.7**	87.2	53.2	88.8*	50.9*	85.7
	Hap-II	55.2	89.6	49.9	87.4	50.1	84.9	51.7	84.8	54.1	87.4
RoSuAr	Hap-I	43.7	44.7	42.8	43.5	43.5	43.9	45.7*	45.4	43.3	45.0
	Hap-II	43.5	43.2	45.5	47.2	43.3	44.4	41.4	43.1	43.4	43.5
RoDiM	Hap-I	0.50*	0.51	0.51	0.51	0.51	0.52	0.52	0.52	0.49**	0.51
	Hap-II	0.53	0.54	0.52	0.52	0.51	0.51	0.50	0.51	0.53	0.52
RoVol	Hap-I	0.55	0.57	0.55	0.56	0.57	0.58	0.60*	0.59	0.55	0.58
	Hap-II	0.59	0.58	0.60	0.61	0.55	0.56	0.52	0.56	0.57	0.57
MidSen	Hap-I	920	1338*	889	1371	910	1383 T	938	1376	988**	1350
	Hap-II	871	1412	964	1319	884	1327	907	1350	819	1372
SenEnd	Hap-I	1698**	1634**	1735	1676*	1729	1675	1763*	1656	1711	1654
	Hap-II	1801	1712	1701	1601	1733	1641	1694	1665	1747	1665
2019											
GY	Hap-I	4.36	7.75	4.46	7.98	4.338	7.91	4.28	7.90	4.29	7.67 T
	Hap-II	4.38	8.14	4.08	7.57	4.446	7.86	4.48	7.91	4.47	8.14
TGW	Hap-I	30.9	35.4	31.0	36.2	30.9	35.8	30.3	35.5	29.8 T	35.0
	Hap-II	30.4	36.8	29.7	34.6	30.7	36.0	31.0	36.2	31.7	36.8
HD	Hap-I	191*	194*	191*	193*	191*	193	191	194	191	194
	Hap-II	190	192	192	196	192	195	191	194	191	193
HI	Hap-I	0.25	0.30	0.25	0.30	0.254	0.30	0.24*	0.30	0.25	0.30
	Hap-II	0.25	0.31	0.25	0.31	0.248	0.31	0.26	0.31	0.25	0.30
PH	Hap-I	62.9	84.1 T	63.8	85.4	64.0	85.7	65.1	87.1*	63.9	85.2
	Hap-II	64.6	87.4	62.7	84.1	62.6	84.1	62.5	83.9	63.1	85.0
GA	Hap-I	1.69	1.94	1.68	1.94	1.686	1.94	1.65*	1.94	1.69	1.95*
	Hap-II	1.67	1.95	1.69	1.95	1.685	1.93	1.71	1.94	1.67	1.93
RoDiM	Hap-I	0.68	0.73	0.68	0.71	0.674	0.71	0.69	0.70	0.68	0.69*
	Hap-II	0.69	0.70	0.69	0.73	0.700	0.72	0.68	0.72	0.69	0.74
RoDrWtPl	Hap-I	0.51	0.54	0.48	0.50T	0.467	0.49 T	0.52	0.53	0.52	0.55
	Hap-II	0.46	0.50	0.54	0.62	0.522	0.59	0.46	0.51	0.46	0.49
Ro:Sh Ratio	Hap-I	0.062*	0.09	0.06	0.08*	0.055*	0.08	0.06	0.09	0.063T	0.09
	Hap-II	0.051	0.08	0.06	0.10	0.064	0.09	0.06	0.08	0.054	0.08
CT	Hap-I	36.9	29.5	37.2	29.7**	36.9	29.2	36.4	29.2	36.8	29.2
	Hap-II	37.1	29.1	36.2	28.4	37.1	29.8	37.2	29.5	37.1	29.7

Significance levels displayed as ns>.10, T <.10 & > .05, * <.05 >.01, ** <.01, ***<0.001.

Note: Frequency: *PRR73.A1* - early flowering (35) and late flowering (14), *TEF.7A* - lower TGW (39) and high TGW (11), *TaCwi.4A* - high yield in drought (29) and low yield in drought (20), *Dreb1*- drought tolerant (20) and drought susceptible (29), *ISBW11.GY.QTL.CANDIDATE* (GY.QTL) - higher yield (27) and lower yield (23).

4. Discussion

4.1 Grain yield responses to drought and association with phenology

In our experiments, there was a moderately severe drought with yield reducing overall by 3.06 t ha^{-1} (-47%). This is representative of Mediterranean drought effects in semi-arid conditions reported for wheat with reductions of yield typically ca. 30-50% (39). The cultivars responded differently to the drought stress as indicated by the significant irrigation x genotype interaction. Higher yield under IR conditions was associated with greater yield loss under SA conditions amongst the cultivars. From the physiological standpoint, it is not surprising that absolute reduction in yield for a given reduction in water resource is strongly influenced by yield potential (40–42).

Drought had only a small effect on heading date overall, advancing GS59 on average by one day in 2018 and three days in 2019; genotypes responded similarly to drought (Fig. 2). In both SA and IR conditions, HD ranged by 10 days amongst cultivars. Correlations between heading date and grain yield were negatively associated under SA conditions in both years, and there was also a negative association under IR conditions in 2019 although less strong than under SA conditions. Bi-plots for the cross-year mean also confirm these effects. Early flowering has been associated with drought escape in wheat in environments subjected to severe early season drought stress, e.g., in northern Mexico (40). Similarly Worland et al. (43) reported increased yield for *Ppd-D1a* early-flowering NILs by ca. 5% compared to *Ppd-D1b* controls in dry years. Each day's advancement in HD raised yield by 0.11 t ha^{-1}. Soil depth was more than 2 m at the field site with a very low organic matter. Presumably a shorter pre-anthesis phase reduced water uptake in this

phase, so that season-long water uptake was redistributed more favorably with regard to the post-anthesis period. However, in one year a similar negative association between HD and yield was recorded under irrigated conditions. This indicated that the negative association may have been partly associated with advanced flowering leading to cooler prevailing temperatures during grain filling and therefore more calendar days for grain filling (44). (45) showed that during grain filling, an increase in 1ºC mean daily temperature higher than optimum can be responsible for decrease in ca. 2.8 mg of grain weight. Observations regarding flowering time and drought resistance are very much dependent on the exact timing of drought stress and we recognize that the present experiments would need to be repeated over more years before we could conclude with certainty that later heading date overall has a negative effect on yield losses under droughts in Turkey. For example, it may be that there is a trade-off between early flowering and the development of a smaller root system, as suggested by (46).

4.2 Associations between canopy senescence traits and responses to drought

In the present study, greater yield amongst cultivars was associated with higher green area per meter square and NDVI at around heading or anthesis under both drought and irrigated conditions. This likely reflected an association between NDVI and biomass at anthesis and hence grains m^{-2} under both treatments. Genetic variation in GY in wheat has previously been associated with green canopy area duration under drought in wheat (41,47–50), sorghum (51). The role of senescence dynamics - start, end and rate of senescence - is important as they relate to grain filling duration and post-anthesis water and N uptake (50,52). Under irrigated conditions, GY was associated positively with senescence start (SenSt) in 2018. Genotypes having delayed senescence

start later may be able to accumulate more plant nutrients and carbohydrates during grain filing duration resulting in higher yield. Our results suggested that there was source limitation if grain growth even under sufficient soil moisture. This could have been due to some heat stress incurred in the experiments combined with the higher grain number in irrigated conditions leading to source limitation during the later stages of grain filling (53).

One of the objectives of this experiment was to compare the two, NDVI and RGB-based vegetation indexes as methods for measuring canopy green area. We found that the RGB-based vegetation indexes showed better association with GY than NDVI measured with the handheld Trimble GreenSeeker (Trimble Navigation Ltd, USA) and in addition it increase throughput. Better association of grain yield with RGB based vegetation indexes than NDVI was also reported in durum wheat by (26) and (27). The role of cooler canopy at anthesis associated with water uptake and root system for drought tolerance is previously reported (5) and was also observed in this experiment with a negative association between GA at anthesis, NDVI at anthesis and GY with canopy temperature (CT) under SA conditions in 2019.

4.3 Effect of shovelomics root traits on responses to drought

Shovelomics represents a high-throughput phenotyping method for field-grown crops and has been used to quantify genetic variation in root traits in maize (18–20), legumes (54) and barley (21). (22) carried out field shovelomics for durum wheat recombinant inbred lines (RIL) for crown root length, number and angle and reported QTL. In our study we applied a shovelomics methodology for bread wheat to quantify variation in nodal root angle, length, roots plant^{-1} and roots shoot^{-1} and association with GY. In the present study, the range in nodal root angle of 45-65^{o}

474 in the semiarid treatment was similar to that of 42.3-69.2° reported by (22) for the Colosseo ×
475 Lloyd durum wheat mapping population assessed at anthesis in the field under optimum agronomic
476 conditions in Italy. Values under irrigation of 45.0-70.0° were also similar to those reported by
477 (22) under irrigation. The association of shallower root angle with higher GY under irrigated
478 conditions in 2019 was possibly associated with increased root density at shallower depth
479 increased recovery of fertilizer N uptake which is predominately distributed in the top 30 cm of
480 the soil. Shallower roots may also increase uptake of irrigation water leading to more transpiration
481 and cooler canopies, so avoiding heat stress. Generally shallower root angle is associated with
482 shallower root distribution in soil and narrow root angle associated with deeper root distribution
483 in soil (15). In durum wheat, (55) reported 20 to 40% yield advantage under irrigated conditions
484 with the shallowest root types compared to deep root type.

485 (56) reported 46.2% and 68.3% of wheat roots are distributed in upper 15 and 30 cm,
486 respectively. In contrast, a steeper angle would be expected to correlate with relatively deeper roots
487 and greater yield under SA conditions, as has been reported in wheat in Australia (13–15). In our
488 experiments soil depth was more than 2 m. Previous studies in maize found steeper root angle
489 related to increased rooting depth under low nitrogen field environments in the USA and South
490 Africa (18). However, in our results we did not see a significant association between root angle
491 and GY under drought. However, under SA conditions in 2019 there was a positive association
492 between nodal root number per shoot and GY and HI, but no association under IR conditions.
493 These results suggest that the wheat ideotype for drought tolerance may be a plant with relatively
494 few tillers but a high number of nodal roots per shoot associated with steeper roots and increased
495 rooting depth. A field study in Pennsylvania in maize found that reduced nodal roots per plant led
496 to increased root length at depth and 57% higher grain yield under water-stressed conditions (57).

497 Tillering influences carbon partitioning, and there is some evidence that reduced tillering increases
498 rooting depth in wheat (58,59) and rice (60).

499 In 2018 terminal stress was severe as rainfall was lower towards the end of crop season
500 than in 2019 (Table 1). In 2018 under semiarid conditions genotypes which had less root surface
501 area and root volume per plant showed higher yield and biomass. It could be speculated that less
502 surface roots may have been associated with more roots distributed relatively deeper in 2018 under
503 SA conditions. Overall under drought conditions fine roots with smaller root diameter may have
504 advantage in exploring maximum area in soil with less energy invested to grow them (61).
505 Whereas in 2019, when terminal drought was less severe, this association with root surface area
506 and volume was not observed.

507 Shovelomics is becoming an increasingly popular method for the high-throughput
508 phenotyping of field-grown crop roots. The shovelomics method we have applied for phenotyping
509 nodal root traits in winter wheat in the present study was shown to be a valuable technique.
510 However, association of canopy temperature with GY indicates that water uptake at depth was
511 contributing to yield increase. As shovelomics traits measures root traits in top 30 cm of soil
512 profile, these technique requires further validation that it is a reliable indicator for roots at depth.
513 Shovelomics is a relatively high-throughput method, making it possible to sample, wash and
514 measure root crowns from 200 plots in two person-days. Shovelomics phenotyping platform is
515 significantly faster the field soil coring, which would take approximately one person-month to
516 sample, wash and extract roots, and image the samples for 200 plots in the present study. This
517 high-throughput shovelomics platform can potentially be used to phenotype large populations to
518 identify QTL, search for candidate genes and develop molecular marker for marker-assisted
519 selection. There are examples of deploying QTL for root depth in other cereal species. In rice, the

520 *Dro1* gene related to steeper crown root angles and deeper rooting was identified by measuring
521 nodal root traits in a high-throughput controlled environment study (62) and has since been used
522 to produce drought tolerant NILs which have been phenotyped in field conditions (63).

523

524 **4.4 Association between molecular markers and responses to drought**

525 Genomic studies using high-throughput genotyping assays like KASP have made it
526 possible to genotype large populations at various loci within a very short time (38). Several recent
527 studies used KASP markers to identify the allelic variation of functional genes in wheat cultivars
528 from China (38), United States (64), and Canada (65). In our study the clear association of *TEF-*
529 *7A* and *TaCwi-4A* with GY and *Dreb1* with root surface area (RoSuAr) under SA conditions
530 indicated the usefulness of deploying these markers in wheat breeding for drought tolerance.

531 Dehydration responsive element binding proteins, *Dreb1*, have been induced by water
532 stress, low temperature and salinity (66). In this study, *TaDreb1* was associated with increased
533 root surface area, root volume and delayed end of senescence which indicated multi-trait effects
534 of this transcription factor which were not previously reported. The *TaCwi-4A* marker was
535 associated with GY, root shot ratio (Ro:Sh ratio) and PH under SA conditions. It was previously
536 reported that storage carbohydrate accumulation in drought susceptible and tolerant cultivars
537 depends on the expression of gene for cell wall invertase (*TaCwi*) in anthers (67). The effect of
538 drought on pollen fertility is irreversible and may cause grain loss or yield reduction under drought
539 conditions. Since these genes tightly control sink strength and carbohydrate supply, therefore
540 deployment of favorable alleles of these genes could maintain pollen fertility and grain number in
541 wheat. The drought tolerance and association of yield-related traits in CIMMYT winter wheat

542 germplasm was strongly associated with the presence of the favorable allele of *TaCwi-4A* which
543 ultimately increased the grain sink size during drought stress. The presence of favorable allele
544 for *TaCwi-4A* gene can enhance the selection accuracy of drought-tolerant germplasm in marker-
545 assisted breeding. Similarly, the association of several important traits like SenEnd, GY, HD, and
546 GA with the flowering time related gene *PRR73-A1* is interesting and indicated the expanded role
547 of these genes in plant development. Previously, Zhang et al (2016), identified that *PRR73-A1* was
548 associated with plant height and explained up to 7.5% of the total phenotyping variability in
549 Chinese wheats. This gene also showed association with plant height in this experiment in 2018.
550 It was previously observed that flowering time related genes are very important for wheat
551 adaptability in target environments, and these genes are associated with several yield component
552 traits (37). Our results provided a set of target genes which could be manipulated to further fine-
553 tune the expression of important drought-tolerance traits.

554

555 ## Conclusion

556 In the Mediterranean environment wheat is grown mostly under semiarid conditions and
557 frequent drought effects wheat yield severely. The strategy of developing drought-tolerant wheat
558 varieties depends on understanding and identifying below-ground and above-ground traits for
559 drought tolerance together with use of marker-assisted selection. In this experiment we used high-
560 throughput phenotyping techniques for characterizing root system architectural and canopy
561 senescence dynamic traits. We conclude that higher number of crown roots per shoot was a key
562 trait for yield increase under drought conditions. Use of RGB-based vegetation index to
563 characterise the canopy green area dynamics could save time and increase precision in selection.

564 Strong association of green area index with GY at flowering was encouraging and this index can
565 be used as tool for early stage selection for higher GY. In this experiment we have evaluated five
566 established functional genes as these genes were associated with different drought-tolerance traits
567 in the field experiments. Genetic marker *TaCwi.4A,* responsible for drought tolerant was associated
568 with higher GY in drought condition in this experiment and can be used for future breeding.
569 Overall, We also provided new insight on effects of root phenotypes and physiological traits, for
570 example the importance of root angle under irrigated conditions and roots per shoot under drought
571 for increasing grain yield which could be important for developing drought-tolerant cultivars.

572

573 ## Acknowledgments

574 CIMMYT-Turkey is supported by the CGIAR Research Program on Wheat and the Republic of
575 Turkey Ministry of Agriculture and Forestry. CIMMYT thanks the Bill and Melinda Gates
576 Foundation (BMGF) and the UK Department for International Development (DFID) for providing
577 financial support through the grant OPP1133199 to AM. We also like to acknowledge Emel OZER
578 and Adam for sowing the experiment, Jose Luis Araus Ortega and Jose Armando Fernández from
579 the University of Barcelona for providing the training for image analysis software to author.

580

581 ## References:

582 1. Le Treut H. Historical overview of climate change. Climate Change 2007: The Physical
583 Science Basis. Contribution of Working Group I to the Fourth Assessment Report of the
584 Intergovernmental Panel on Climate Change. Cambridge University Press; 2007.

585 2. Trnka M, Feng S, Semenov MA, Olesen JE, Kersebaum KC, Rötter RP, et al. Mitigation
586 efforts will not fully alleviate the increase in water scarcity occurrence probability in
587 wheat-producing areas. Sci Adv [Internet]. 2019 Sep 1;5(9):eaau2406. Available from:
588 http://advances.sciencemag.org/content/5/9/eaau2406.abstract

589 3. Leng G, Hall J. Crop yield sensitivity of global major agricultural countries to droughts
590 and the projected changes in the future. Sci Total Environ [Internet]. 2019;654:811–21.
591 Available from: http://www.sciencedirect.com/science/article/pii/S0048969718343341

592 4. Reynolds M, Dreccer F, Trethowan R. Drought-adaptive traits derived from wheat wild
593 relatives and landraces. J Exp Bot. 2007;58(2):177–86.

594 5. Lopes MS, Reynolds MP. Partitioning of assimilates to deeper roots is associated with
595 cooler canopies and increased yield under drought in wheat. Funct Plant Biol [Internet].
596 2010;37(2):147–56. Available from: https://doi.org/10.1071/FP09121

597 6. Foulkes MJ, Hawkesford MJ, Barraclough PB, Holdsworth MJ, Kerr S, Kightley S, et al.
598 Identifying traits to improve the nitrogen economy of wheat: Recent advances and future
599 prospects. F Crop Res. 2009 Dec 12;114(3):329–42.

600 7. Lopes MS, Reynolds MP. Stay-green in spring wheat can be determined by spectral
601 reflectance measurements (normalized difference vegetation index) independently from
602 phenology. J Exp Bot. 2012;63(10):3789–98.

603 8. Gregory PJ, McGowan M, Biscoe P V, Hunter B. Water relations of winter wheat: 1.
604 Growth of the root system. J Agric Sci. 1978;91(1):91–102.

605 9. Wasson AP, Richards RA, Chatrath R, Misra SC, Prasad SVS, Rebetzke GJ, et al. Traits

606 and selection strategies to improve root systems and water uptake in water-limited wheat
607 crops. J Exp Bot. 2012;63(9):3485–98.

608 10. Lynch JP. Steep, cheap and deep: an ideotype to optimize water and N acquisition by
609 maize root systems. Ann Bot. 2013;112(2):347–57.

610 11. Richard CAI, Hickey LT, Fletcher S, Jennings R, Chenu K, Christopher JT. High-
611 throughput phenotyping of seminal root traits in wheat. Plant Methods. 2015;11(1):1–11.

612 12. van Noordwijk M. Functional interpretation of root densities in the field for nutrient and
613 water uptake. Instituut voor Bodemvruchtbaarheid; 1983.

614 13. Olivares-Villegas JJ, Reynolds MP, McDonald GK. Drought-adaptive attributes in the
615 Seri/Babax hexaploid wheat population. Funct Plant Biol. 2007;34(3):189–203.

616 14. Manschadi AM, Hammer GL, Christopher JT, Devoil P. Genotypic variation in seedling
617 root architectural traits and implications for drought adaptation in wheat (Triticum
618 aestivum L.). Plant Soil. 2008;303(1–2):115–29.

619 15. Manschadi AM, Christopher JT, Hammer GL, Devoil P. Experimental and modelling
620 studies of drought-adaptive root architectural traits in wheat (Triticum aestivum L.). Plant
621 Biosyst. 2010;144(2):458–62.

622 16. Fiorani F, Schurr U. Future scenarios for plant phenotyping. Annu Rev Plant Biol.
623 2013;64:267–91.

624 17. Köpke U. Ein Vergleich von Feldmethoden zur Bestimmung des Wurzelwachstums
625 landwirtschaftlicher Kulturpflanzen. Doctoral thesis, Univ. Göttingen. 1979.

626 18. Trachsel S, Kaeppler SM, Brown KM, Lynch JP. Shovelomics: high throughput

627 phenotyping of maize (Zea mays L.) root architecture in the field. Plant Soil. 2011;341(1–
628 2):75–87.

629 19. Lynch JP. Root phenes for enhanced soil exploration and phosphorus acquisition: tools for
630 future crops. Plant Physiol. 2011;156(3):1041–9.

631 20. Abiven S, Hund A, Martinsen V, Cornelissen G. Biochar amendment increases maize root
632 surface areas and branching: a shovelomics study in Zambia. Plant Soil. 2015;395(1–
633 2):45–55.

634 21. Wojciechowski T, Putz A, Schurr U, Federau J, Fiorani F, Briese C, et al. Root
635 phenotyping of temperate cereals–a high throughput phenotyping pipeline for field
636 experiments. In: International Society of Root Research Symposium.
637 Pflanzenwissenschaften; 2015.

638 22. Maccaferri M, El-Feki W, Nazemi G, Salvi S, Canè MA, Colalongo MC, et al. Prioritizing
639 quantitative trait loci for root system architecture in tetraploid wheat. J Exp Bot.
640 2016;67(4):1161–78.

641 23. York LM, Slack S, Bennett MJ, Foulkes MJ. Wheat shovelomics I: A field phenotyping
642 approach for characterising the structure and function of root systems in tillering species.
643 BioRxiv. 2018;280875.

644 24. Tucker CJ. Red and photographic infrared linear combinations for monitoring vegetation.
645 Remote Sens Environ. 1979;8(2):127–50.

646 25. Rouse Jr JW. Monitoring the vernal advancement and retrogradation (green wave effect)
647 of natural vegetation. 1973;

26. Kefauver SC, El-Haddad G, Vergara O, Araus JL, Kefauver SC, Vergara-Diaz O, et al. RGB picture vegetation indexes for High-Throughput Phenotyping Platforms (HTPPs). 2015;

27. Fernandez-Gallego JA, Kefauver SC, Vatter T, Gutiérrez NA, Nieto-Taladriz MT, Araus JL. Low-cost assessment of grain yield in durum wheat using RGB images. Eur J Agron. 2019;105:146–56.

28. Liu Q, Zhao N, Yamaguch-Shinozaki K, Shinozaki K. Regulatory role of DREB transcription factors in plant drought, salt and cold tolerance. Chinese Sci Bull [Internet]. 2000;45(11):970–5. Available from: https://doi.org/10.1007/BF02884972

29. Zheng J, Liu H, Wang Y, Wang L, Chang X, Jing R, et al. TEF-7A, a transcript elongation factor gene, influences yield-related traits in bread wheat (Triticum aestivum L.). J Exp Bot [Internet]. 2014 Oct 1;65(18):5351–65. Available from: https://doi.org/10.1093/jxb/eru306

30. Wang H, Wang S, Chang X, Hao C, Sun D, Jing R. Identification of TaPPH-7A haplotypes and development of a molecular marker associated with important agronomic traits in common wheat. BMC Plant Biol [Internet]. 2019;19(1):296. Available from: https://doi.org/10.1186/s12870-019-1901-0

31. Zhang W, Zhao G, Gao L, Kong X, Guo Z, Wu B, et al. Functional Studies of Heading Date-Related Gene TaPRR73, a Paralog of Ppd1 in Common Wheat. Front Plant Sci [Internet]. 2016 Jun 1;7:772. Available from: https://pubmed.ncbi.nlm.nih.gov/27313595

32. Ma D, Yan J, He Z, Wu L, Xia X. Characterization of a cell wall invertase gene TaCwi-A1 on common wheat chromosome 2A and development of functional markers. Mol

Breed [Internet]. 2012;29(1):43–52. Available from: https://doi.org/10.1007/s11032-010-9524-z

33. York LM, Lynch JP. Intensive field phenotyping of maize (Zea mays L.) root crowns identifies phenes and phene integration associated with plant growth and nitrogen acquisition. J Exp Bot. 2015;66(18):5493–505.

34. Schneider CA, Rasband WS, Eliceiri KW. NIH Image to ImageJ: 25 years of image analysis. Nat Methods. 2012;9(7):671–5.

35. Casadesus J, Villegas D. Conventional digital cameras as a tool for assessing leaf area index and biomass for cereal breeding. J Integr Plant Biol. 2014;56(1):7–14.

36. Dreisigacker S, Tiwari R, Sheoran S. Laboratory manual: ICAR-CIMMYT molecular breeding course in wheat. In ICAR; 2013.

37. Khalid M, Afzal F, Gul A, Amir R, Subhani A, Ahmed Z, et al. Molecular characterization of 87 functional genes in wheat diversity panel and their association with phenotypes under well-watered and water-limited conditions. Front Plant Sci. 2019;10:717.

38. Rasheed A, Wen W, Gao F, Zhai S, Jin H, Liu J, et al. Development and validation of KASP assays for genes underpinning key economic traits in bread wheat. Theor Appl Genet. 2016;129(10):1843–60.

39. Giunta F, Motzo R, Deidda M. Effect of drought on yield and yield components of durum wheat and triticale in a Mediterranean environment. F Crop Res. 1993 Jun 1;33(4):399–409.

691 40. Fischer RA, Maurer R. Drought resistance in spring wheat cultivars. I. Grain yield
692 responses. Aust J Agric Res. 1978;29(5):897–912.

693 41. Foulkes MJ, Sylvester-Bradley R, Weightman R, Snape JW. Identifying physiological
694 traits associated with improved drought resistance in winter wheat. F Crop Res.
695 2007;103(1):11–24.

696 42. Kumar BNA, Azam-Ali SN, Snape JW, Weightman RM, Foulkes MJ. Relationships
697 between carbon isotope discrimination and grain yield in winter wheat under well-watered
698 and drought conditions. J Agric Sci. 2011;149(3):257–72.

699 43. Worland AJ, Börner A, Korzun V, Li WM, Petrovic S, Sayers EJ. The influence of
700 photoperiod genes on the adaptability of European winter wheats. Euphytica. 1998;100(1–
701 3):385–94.

702 44. Wu X, Tang Y, Li C, Wu C. Characterization of the rate and duration of grain filling in
703 wheat in southwestern China. Plant Prod Sci. 2018;21(4):358–69.

704 45. Brdar MD, Kraljević-Balalić MM, Kobiljski BĐ. The parameters of grain filling and yield
705 components in common wheat (Triticum aestivum L.) and durum wheat (Triticum
706 turgidum L. var. durum). Cent Eur J Biol. 2008;3(1):75–82.

707 46. Foulkes MJ, Sylvester-Bradley R, Worland AJ, Snape JW. Effects of a photoperiod-
708 response gene Ppd-D1 on yield potential and drought resistance in UK winter wheat.
709 Euphytica. 2004;135(1):63–73.

710 47. Gorny AG, Garczynski S. Genotypic and nutrition-dependent variation in water use
711 efficiency and photosynthetic activity of leaves in winter wheat (Triticum aestivum L.). J

712 Appl Genet. 2002;43(2):145–60.

713 48. Verma V, Foulkes MJ, Worland AJ, Sylvester-Bradley R, Caligari PDS, Snape JW.
714 Mapping quantitative trait loci for flag leaf senescence as a yield determinant in winter
715 wheat under optimal and drought-stressed environments. Euphytica. 2004;135(3):255–63.

716 49. Christopher JT, Manschadi AM, Hammer GL, Borrell AK. Developmental and
717 physiological traits associated with high yield and stay-green phenotype in wheat. Aust J
718 Agric Res. 2008;59(4):354–64.

719 50. Nehe AS, Misra S, Murchie EH, Chinnathambi K, Tyagi B, Foulkes MJ. Nitrogen
720 partitioning and remobilization in relation to leaf senescence, grain yield and protein
721 concentration in Indian wheat cultivars. F Crop Res. 2020;

722 51. Borrell AK, Hammer GL, Henzell RG. Does maintaining green leaf area in sorghum
723 improve yield under drought? II. Dry matter production and yield. Crop Sci.
724 2000;40(4):1037–48.

725 52. Nehe A, Akin B, Sanal T, Evlice AK, Ünsal R, Dinçer N, et al. Genotype x environment
726 interaction and genetic gain for grain yield and grain quality traits in Turkish spring wheat
727 released between 1964 and 2010. PLoS One. 2019 Jul 18;14(7):e0219432.

728 53. Nehe AS, Misra S, Murchie EH, Chinnathambi K, Foulkes MJ. Genetic variation in N-use
729 efficiency and associated traits in Indian wheat cultivars. F Crop Res [Internet].
730 2018;225(June):152–62. Available from: https://doi.org/10.1016/j.fcr.2018.06.002

731 54. Burridge J, Jochua CN, Bucksch A, Lynch JP. Legume shovelomics: high—throughput
732 phenotyping of common bean (Phaseolus vulgaris L.) and cowpea (Vigna unguiculata

733 subsp, unguiculata) root architecture in the field. F Crop Res. 2016;192:21–32.

734 55. El Hassouni K, Alahmad S, Belkadi B, Filali-Maltouf A, Hickey LT, Bassi FM. Root
735 system architecture and its association with yield under different water regimes in durum
736 wheat. Crop Sci. 2018;58(6):2331–46.

737 56. Fan J, McConkey B, Wang H, Janzen H. Root distribution by depth for temperate
738 agricultural crops. F Crop Res [Internet]. 2016;189:68–74. Available from:
739 http://www.sciencedirect.com/science/article/pii/S0378429016300399

740 57. Gao Y, Lynch JP. Reduced crown root number improves water acquisition under water
741 deficit stress in maize (Zea mays L.). J Exp Bot. 2016;67(15):4545–57.

742 58. Duggan BL, Richards RA, Van Herwaarden AF. Agronomic evaluation of a tiller
743 inhibition gene (tin) in wheat. II. Growth and partitioning of assimilate. Aust J Agric Res.
744 2005;56(2):179–86.

745 59. Richards RA. Physiological traits used in the breeding of new cultivars for water-scarce
746 environments. Agric water Manag. 2006;80(1–3):197–211.

747 60. Yoshida S, Hasegawa S. The rice root system: its development and function. Drought
748 Resist Crop with Emphas rice. 1982;10:97–134.

749 61. Wasaya A, Zhang X, Fang Q, Yan Z. Root phenotyping for drought tolerance: a review.
750 Agronomy. 2018;8(11):241.

751 62. Uga Y, Okuno K, Yano M. Dro1, a major QTL involved in deep rooting of rice under
752 upland field conditions. J Exp Bot. 2011;62(8):2485–94.

753 63. Uga Y, Sugimoto K, Ogawa S, Rane J, Ishitani M, Hara N, et al. Control of root system

754 architecture by DEEPER ROOTING 1 increases rice yield under drought conditions. Nat
755 Genet. 2013;45(9):1097–102.

756 64. Grogan SM, Brown-Guedira G, Haley SD, McMaster GS, Reid SD, Smith J, et al. Allelic
757 variation in developmental genes and effects on winter wheat heading date in the US
758 Great Plains. PLoS One. 2016;11(4):e0152852.

759 65. Perez-Lara E, Semagn K, Chen H, Ciechanowska I, Iqbal M, N'Diaye A, et al. Allelic
760 variation and effects of 16 candidate genes on disease resistance in western Canadian
761 spring wheat cultivars. Mol Breed. 2017;37(3):23.

762 66. Zhang J, Dell B, Conocono E, Waters I, Setter T, Appels R. Water deficits in wheat:
763 fructan exohydrolase (1-FEH) mRNA expression and relationship to soluble carbohydrate
764 concentrations in two varieties. New Phytol. 2009;181(4):843–50.

765 67. Shen Y-G, Zhang W-K, He S-J, Zhang J-S, Liu Q, Chen S-Y. An EREBP/AP2-type
766 protein in Triticum aestivum was a DRE-binding transcription factor induced by cold,
767 dehydration and ABA stress. Theor Appl Genet. 2003;106(5):923–30.

768

(a)

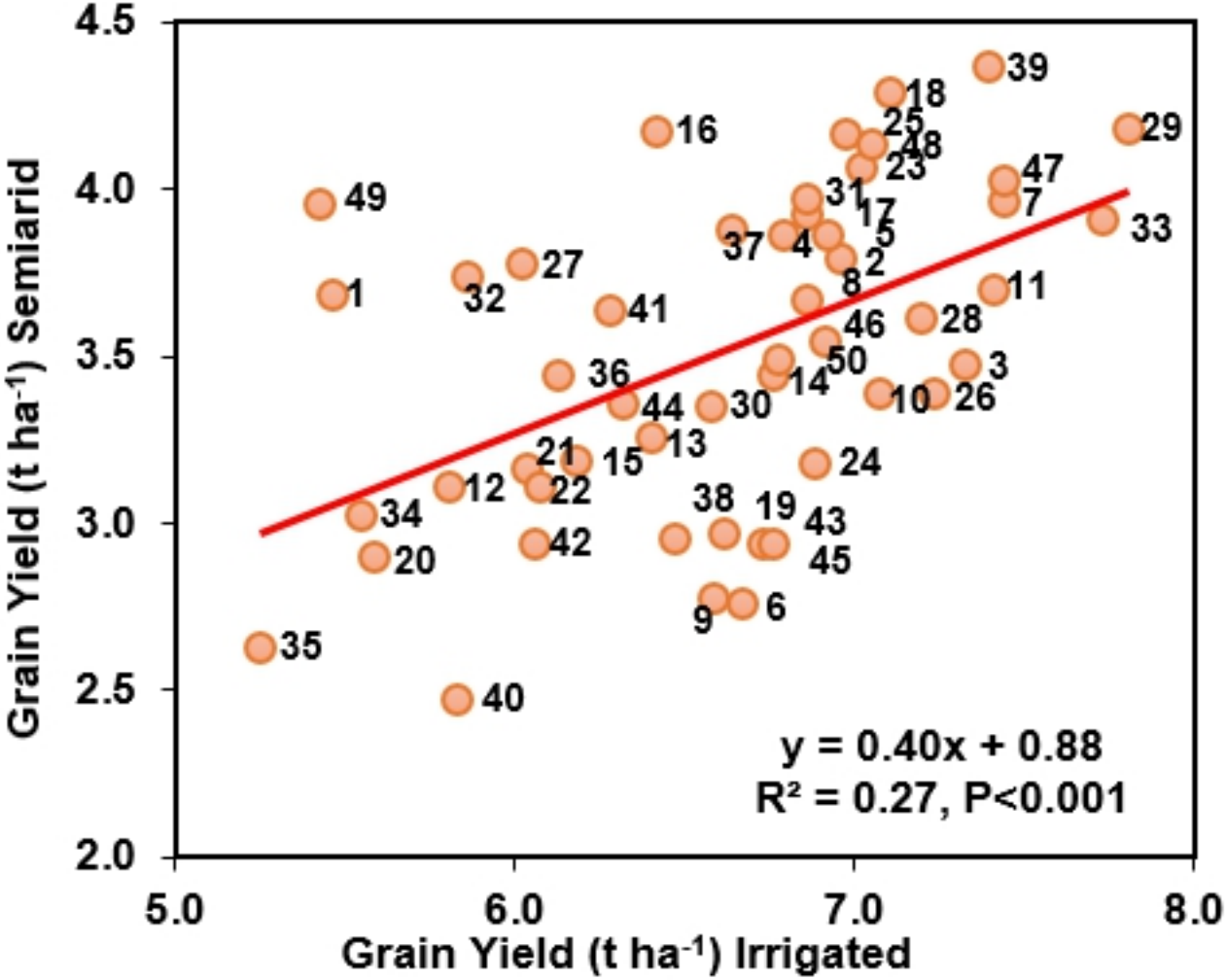
Grain Yield (t ha-1) Semiarid
Grain Yield (t ha-1) Irrigated
y = 0.40x + 0.88
R² = 0.27, P<0.001
4.5
4.0
3.5
3.0
2.5
2.0
5.0
6.0
7.0
8.0
39
18
25
48
16
29
23
47
49
31
17
7
33
37
4
5
27
2
1
32
8
11
41
46
28
36
50
3
14
44
30
10
26
21
13
15
24
12
22
38
19
43
34
42
45
20
9
6
35
40

Fig 1 a

(b)

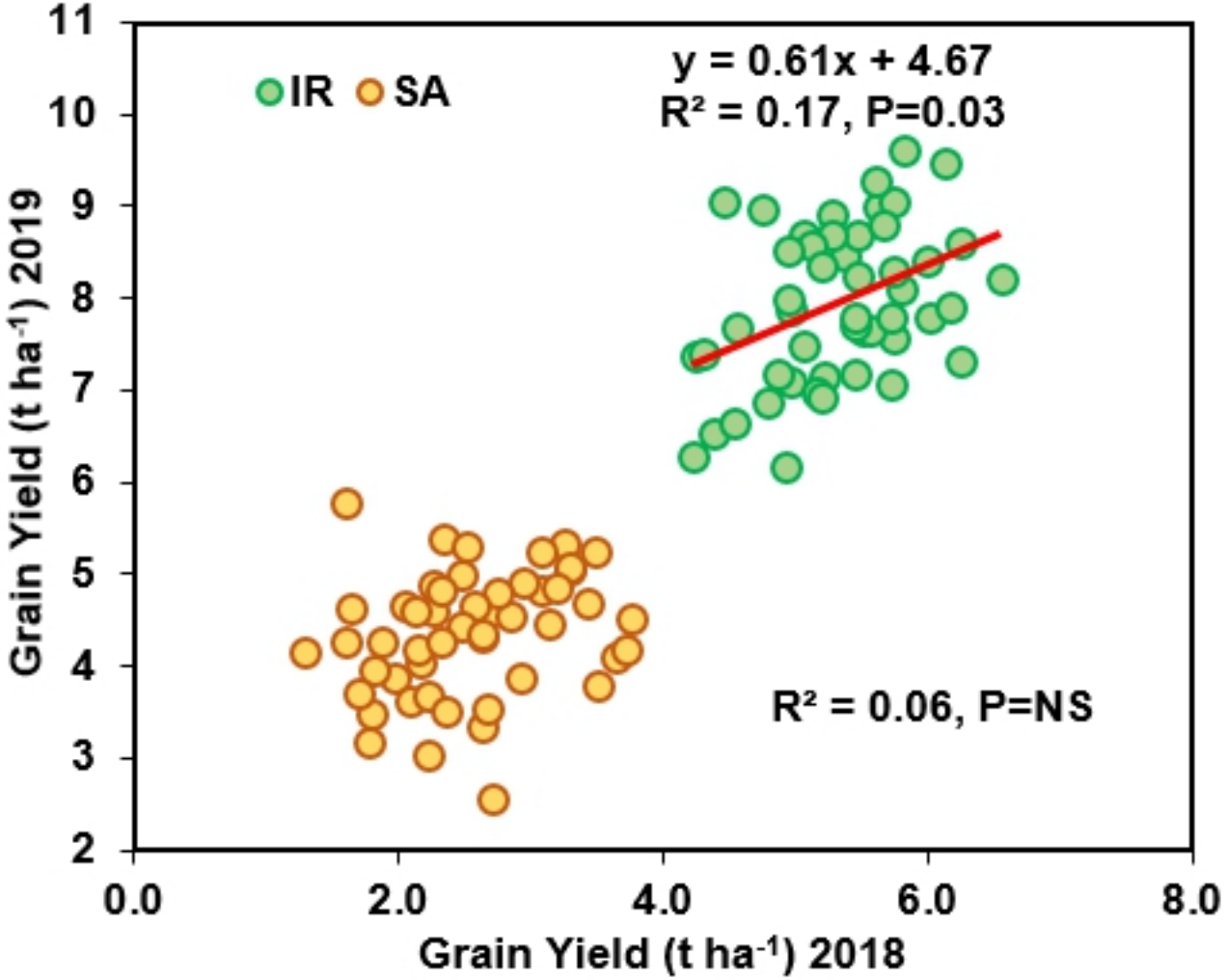
IR
SA
y = 0.61x + 4.67
R² = 0.17, P=0.03
R² = 0.06, P=NS
Grain Yield (t ha-1) 2019
Grain Yield (t ha-1) 2018
11
10
9
8
7
6
5
4
3
2
0.0
2.0
4.0
6.0
8.0

Fig 1 b

(a)

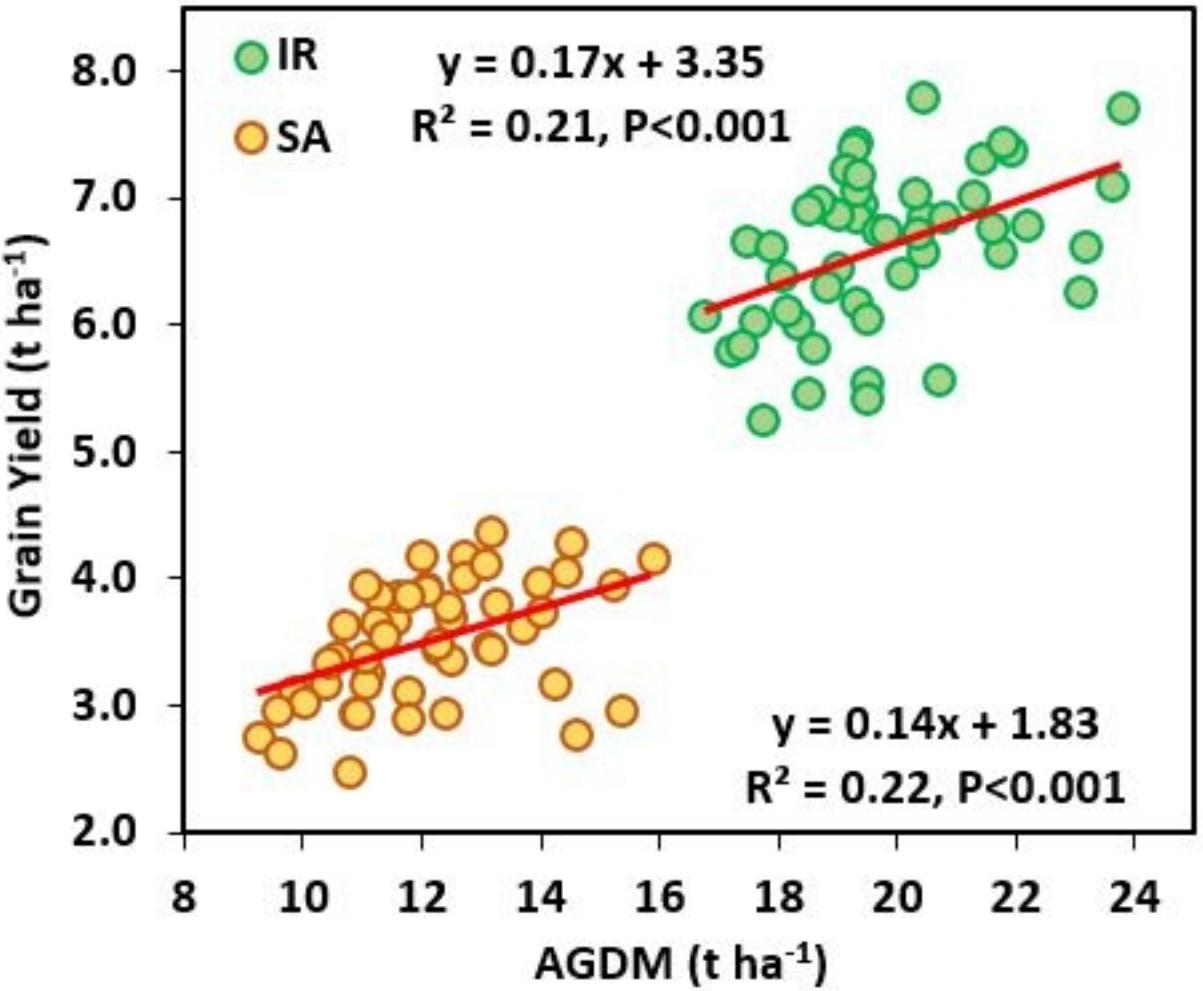
IR
SA
y = 0.17x + 3.35
R² = 0.21, P<0.001
y = 0.14x + 1.83
R² = 0.22, P<0.001
Grain Yield (t ha-1)
AGDM (t ha-1)
8.0
7.0
6.0
5.0
4.0
3.0
2.0
8
10
12
14
16
18
20
22
24

Fig 2 a

(b)

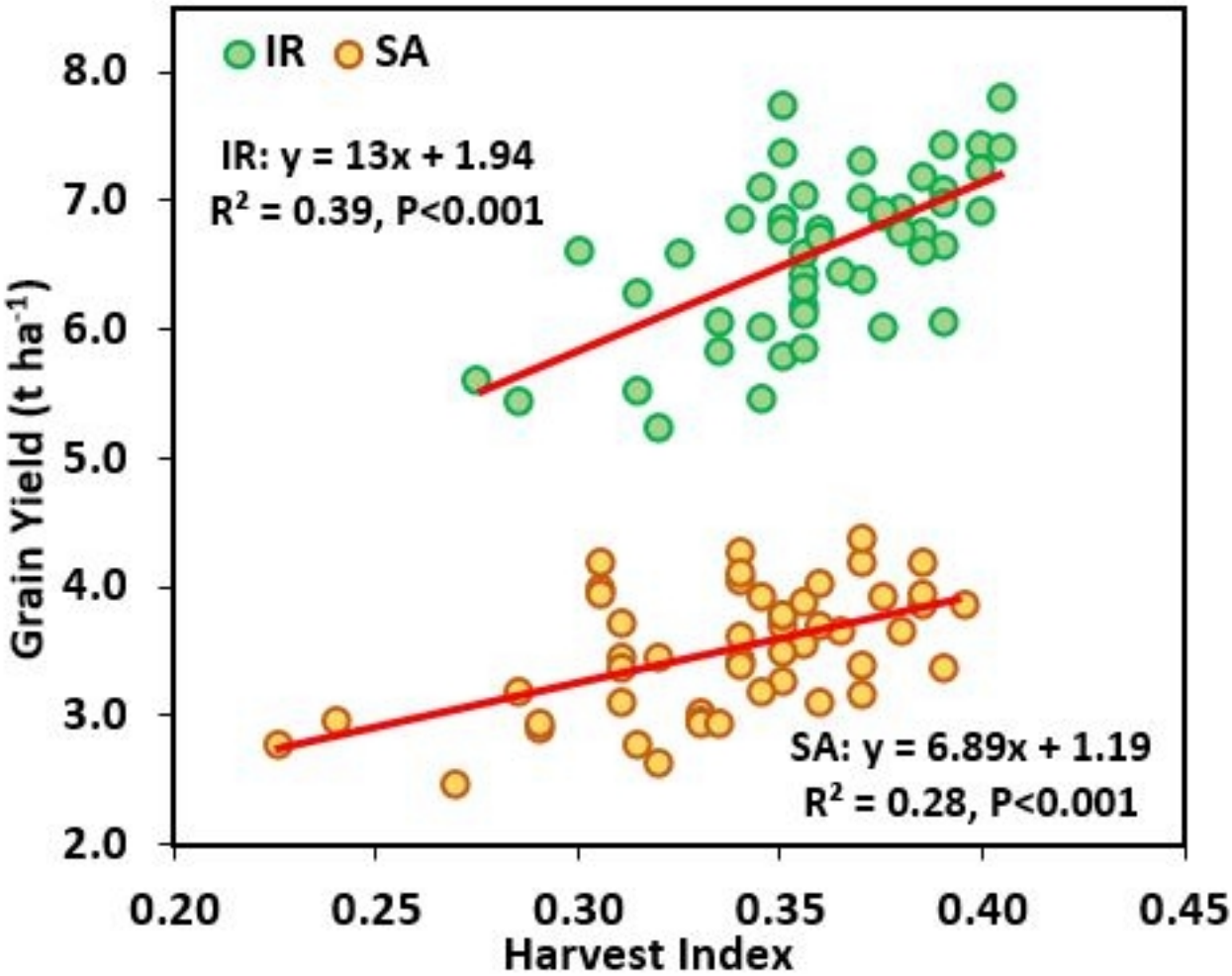
IR
SA
IR: y = 13x + 1.94
R² = 0.39, P<0.001
SA: y = 6.89x + 1.19
R² = 0.28, P<0.001
Grain Yield (t ha-1)
8.0
7.0
6.0
5.0
4.0
3.0
2.0
0.20
0.25
0.30
0.35
0.40
0.45
Harvest Index

Fig 2 b

(c)

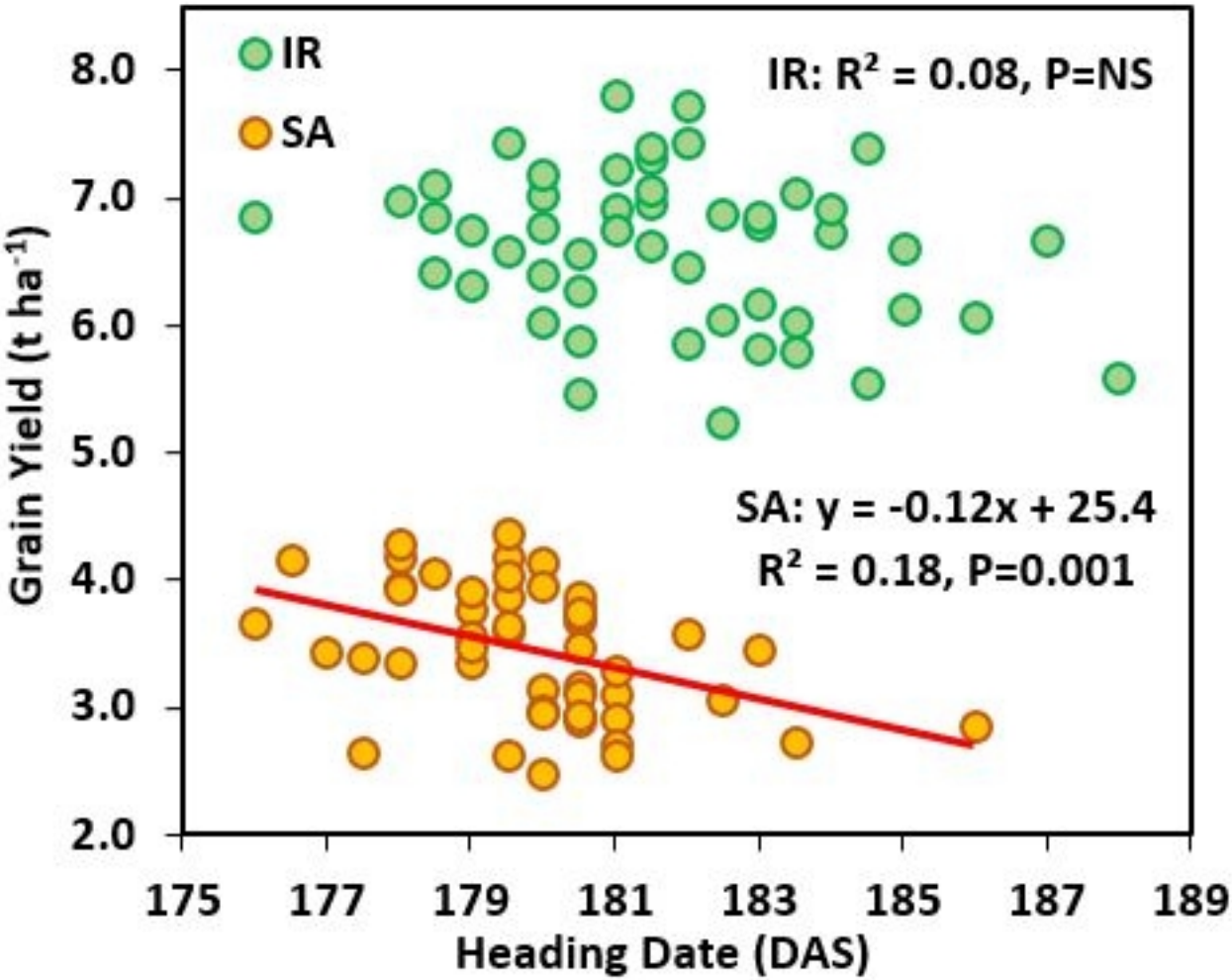
IR
SA
IR: R² = 0.08, P=NS
SA: y = -0.12x + 25.4
R² = 0.18, P=0.001
Grain Yield (t ha-1)
8.0
7.0
6.0
5.0
4.0
3.0
2.0
175
177
179
181
183
185
187
189
Heading Date (DAS)

Fig 2 c

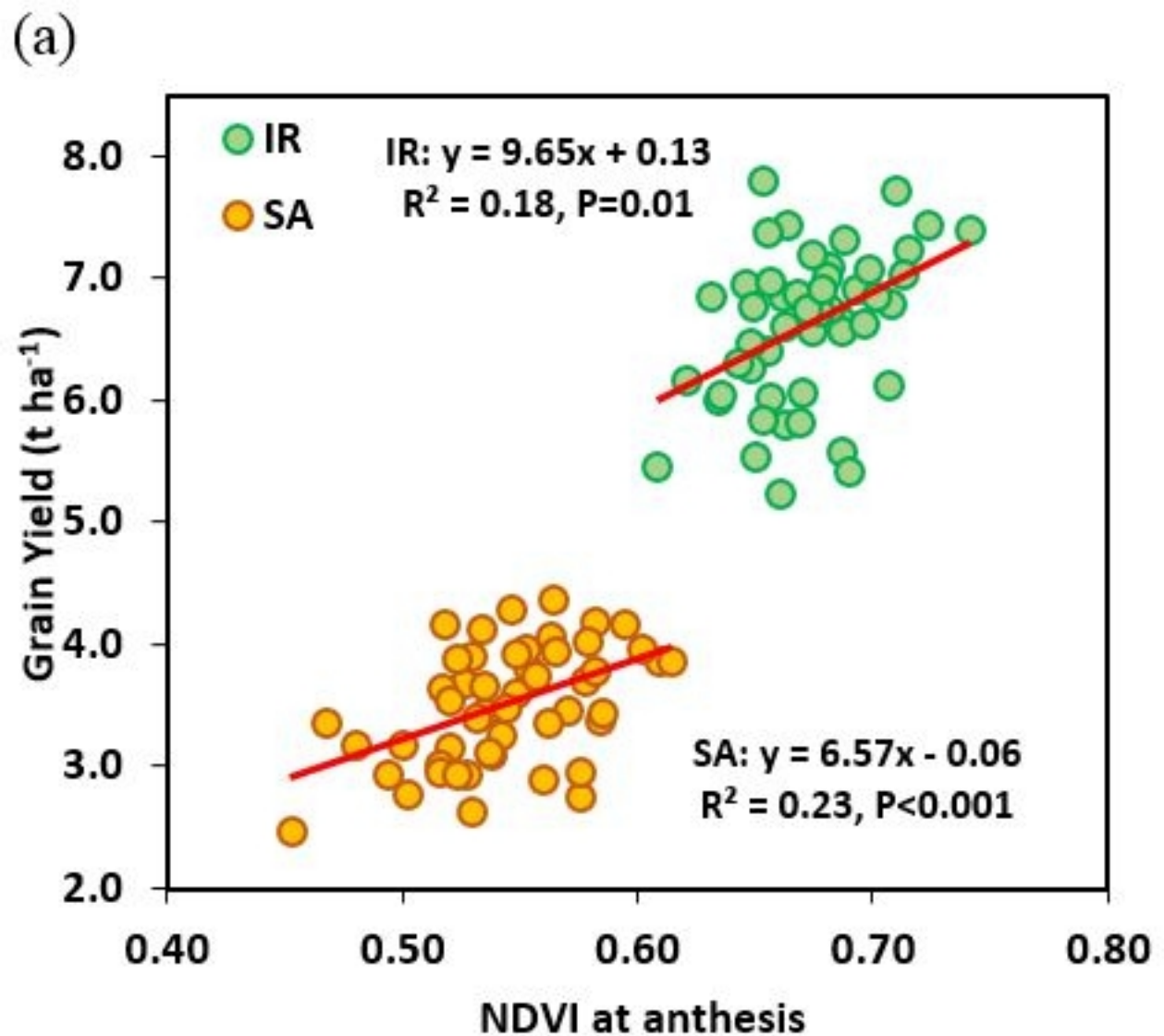
(a)
IR
SA
IR: y = 9.65x + 0.13
R² = 0.18, P=0.01
SA: y = 6.57x - 0.06
R² = 0.23, P<0.001
Grain Yield (t ha-1)
8.0
7.0
6.0
5.0
4.0
3.0
2.0
0.40
0.50
0.60
0.70
0.80
NDVI at anthesis

Fig 3 a

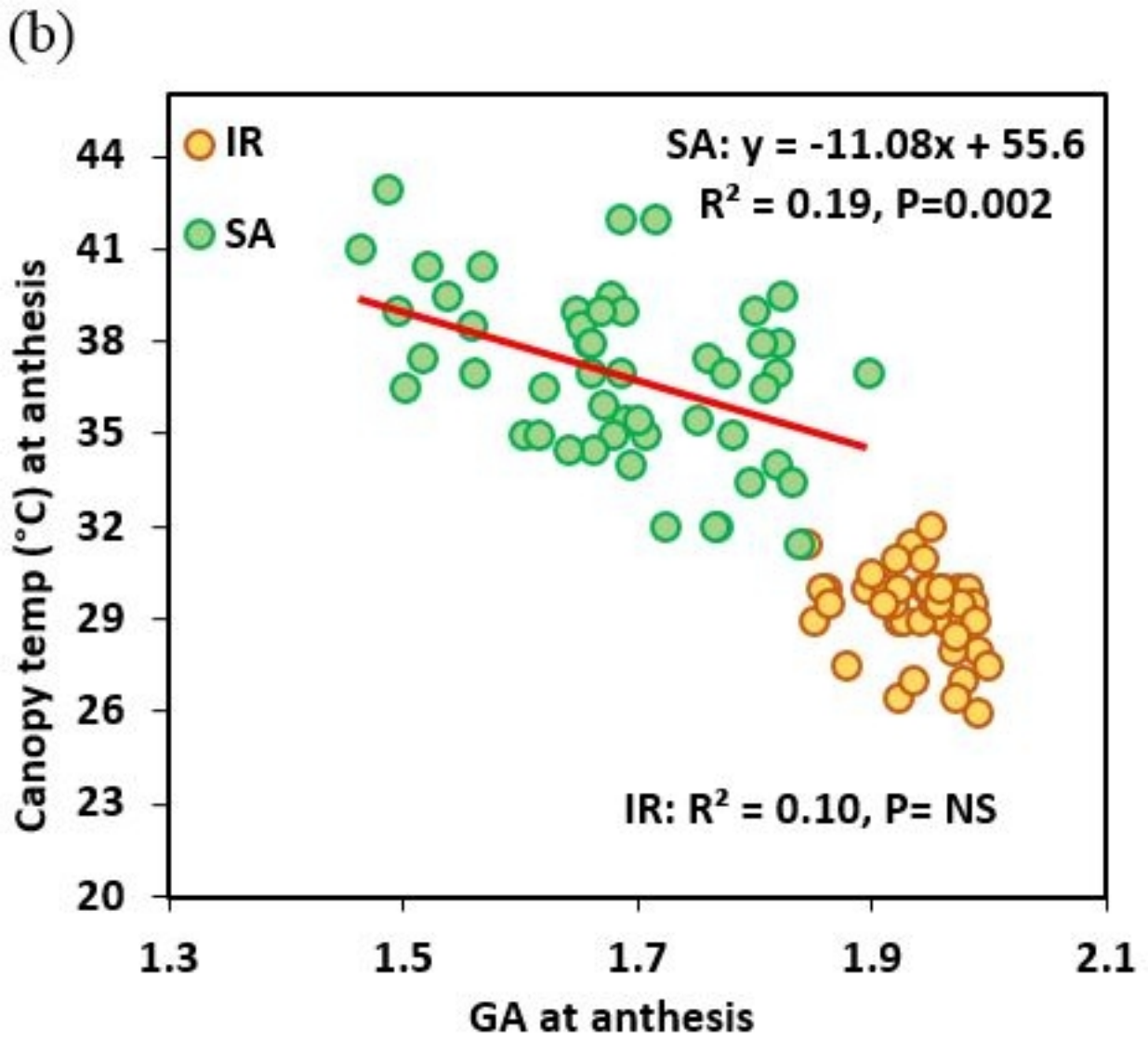
(b)
IR
SA
SA: y = -11.08x + 55.6
R² = 0.19, P=0.002
IR: R² = 0.10, P= NS
Canopy temp (°C) at anthesis
GA at anthesis
44
41
38
35
32
29
26
23
20
1.3
1.5
1.7
1.9
2.1

Fig 3 b

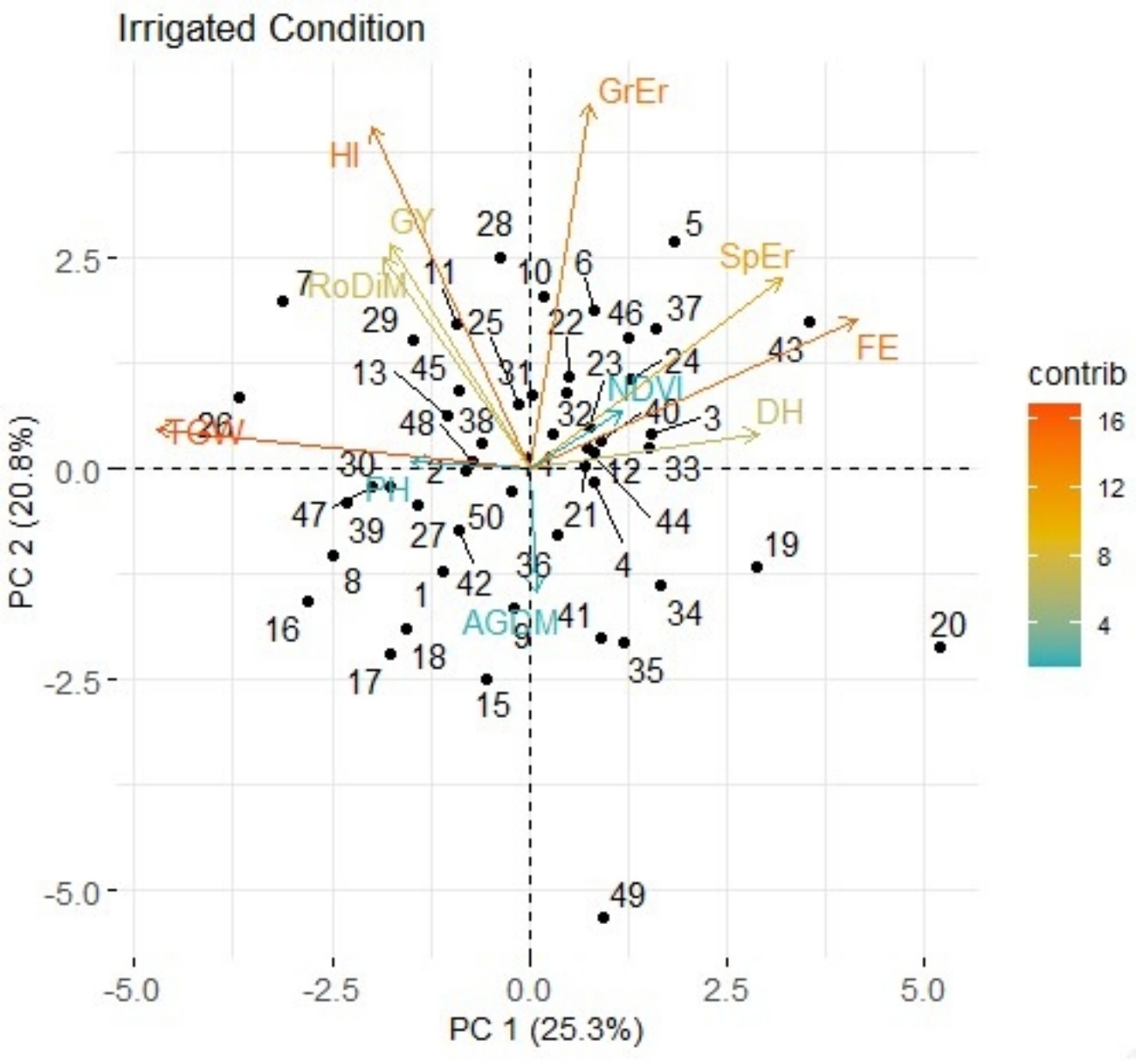

Fig 4 Irrigated

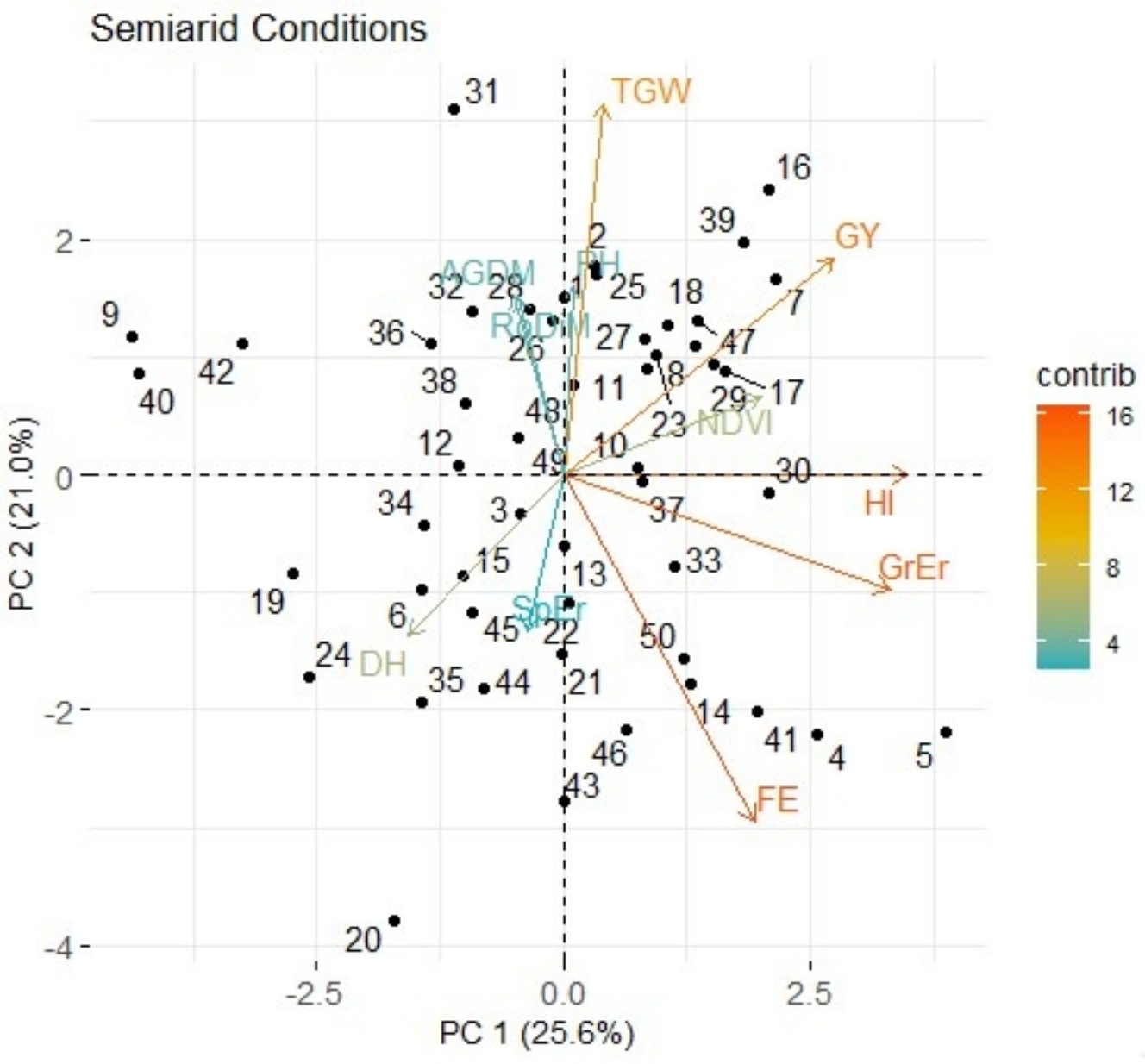

Fig 4 Semiarid

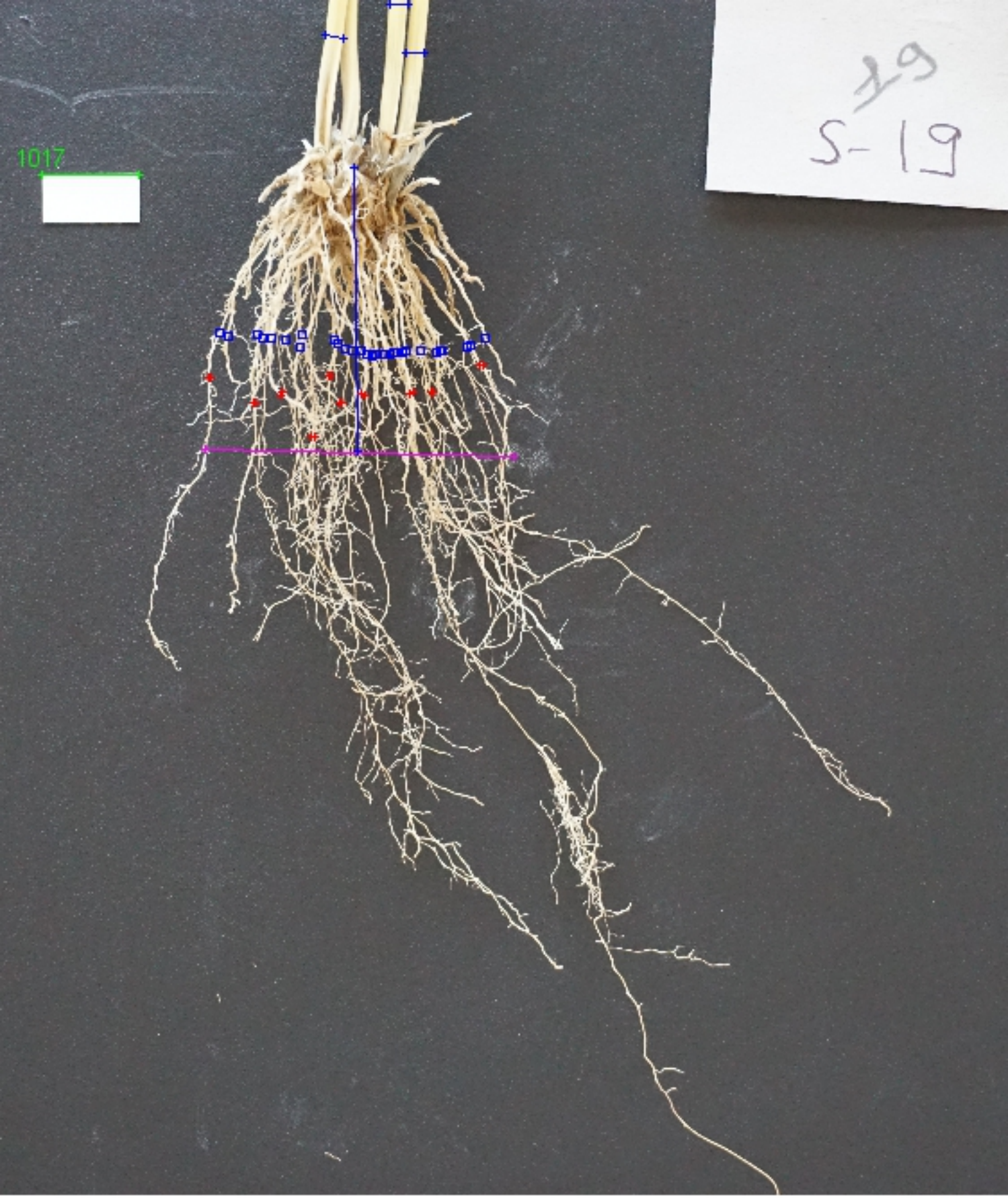

S Fig 1 a

S Fig 1 b